

CURVATURE ALIGNED SIMPLEX GRADIENT: PRINCIPLED SAMPLE SET CONSTRUCTION FOR NUMERICAL DIFFERENTIATION

DANIEL LENGYEL, PANOS PARPAS

Department of Computing, Imperial College London

NIKOLAS KANTAS

Department of Mathematics, Imperial College London

NICHOLAS R. JENNINGS

Loughborough University

ABSTRACT. The simplex gradient, a popular numerical differentiation method due to its flexibility, lacks a principled method by which to construct the sample set, specifically the location of function evaluations. Such evaluations, especially from real-world systems, are often noisy and expensive to obtain, making it essential that each evaluation is carefully chosen to reduce cost and increase accuracy. This paper introduces the curvature aligned simplex gradient (CASG), which provably selects the optimal sample set under a mean squared error objective. As CASG requires function-dependent information often not available in practice, we additionally introduce a framework which exploits a history of function evaluations often present in practical applications. Our numerical results, focusing on applications in sensitivity analysis and derivative free optimization, show that our methodology significantly outperforms or matches the performance of the benchmark gradient estimator given by forward differences (FD) which is given exact function-dependent information that is not available in practice. Furthermore, our methodology is comparable to the performance of central differences (CD) that requires twice the number of function evaluations.

1. INTRODUCTION

Gradient estimation is crucial in applications ranging from chemical engineering [2], financial markets [28] to medical and biological research [40, 33]. When it is possible to modify a system, then methods such as automatic differentiation [29, 3, 43], infinitesimal perturbation analysis [47, 50], score function estimators [52] or weak derivative estimators [8] are the first choice for gradient estimation. However, many applications involve expensive physical processes, simulations or legacy code which cannot be easily modified. This is generally the domain of numerical differentiation, where one only has access to potentially corrupted system

E-mail addresses: d.lengyel19@imperial.ac.uk.

Date: January 3, 2025.

function evaluations which may be expensive to obtain. The challenge in such circumstances is determining the optimal points for function evaluation to refine the gradient estimate.

A strong numerical differentiation method that significantly benefits from a careful choice of the sample set, i.e., locations of evaluations, is the simplex gradient. The simplex gradient places limited restrictions on the sample set, which has led to its gain in popularity [31, 32, 41, 5, 18], especially in the derivative-free optimization community [16, 17, 21, 20]. However, there is only a limited understanding of which sample sets may lead to good gradient estimates and how to construct them in practice [32, 31, 41]. In this paper, we present substantial advancements addressing this open question.

1.1. Related Works. Besides a general sample set, there are various other benefits to the use of the simplex gradient. The simplex gradient uses a linear model and hence only requires $d + 1$ function evaluations, with d being the number of input variables. A linear model is often preferable as higher order models can lead to instability [15, 22], which becomes amplified when noise is introduced. Unlike the simplex gradient, such methods then often require a form of explicit regularization [30, 1, 19, 35, 51, 48] which is difficult to choose in practice. The number of function evaluations is also a strong benefit of the simplex gradient. Higher-order methods or methods such as Richardson Extrapolation [14, 13, 35, 11, 24] often require far more evaluations which may be infeasible. Conversely, using fewer points would make the linear fit under-determined and can only be applied in cases where the gradient is sparse [10]. Inexact methods which require fewer than $d + 1$ function evaluations are often stochastic in nature, for example simultaneous perturbation stochastic approximation [46, 45, 7] and smoothing methods [5]. However, such methods are often far too inaccurate for gradient estimation [9] and have been shown to have poorer performance compared to a deterministic counterpart [42, 5, 6].

If a gradient estimator is allowed to use only $d + 1$ function evaluations, the baseline methods are often variations of the simplex gradient, with the variation being in the choice of the sample set. While simple in nature, forward differences has remained the go-to simplex gradient based method as it provides a closed form solution for its optimal sample set [12, 6] and outperforms other comparable methods [12]. However the conditions on the sample set are very restrictive and may hinder performance. Other methods which have allowed for a general sample set are often heuristically derived from general principles from function approximation [22, 14] or have been presented in terms of Design of Experiment (DoE) [53, 12]. DoE was pioneered by [23] to assess the factors influencing the response of a system by laying out principles by which to assess the individual and combined impact of changing parameters to the system in an efficient manner. These methods have resulted in various schemes, such as the fractional factorial design [36] and the Plackett–Burman design [39]. Yet, there is no guarantee or systematic understanding for when these designs will provide good gradient estimates. Additionally their performance is generally comparable to or worse than forward differences [12], making finite difference so far the preferable choice.

To choose a sample set in practice, there is some function-dependent information which is needed as otherwise a sample set cannot be adapted to a specific problem. However, such information is not readily available in practice, and hence many methods have focused on developing such estimators for the use in finite difference schemes [26, 25, 44, 38, 2]. While these methods attempt to reduce the number of function evaluations by estimating the higher-order information only periodically, the procedure remains expensive as more function evaluations than strictly needed for gradient estimation are required.

1.2. Contributions. Against this background we present the following contributions.

- We introduce the Curvature Aligned Simplex Gradient (CASG), a simplex gradient method based on principled sample set construction. CASG minimizes a mean squared error using a Taylor approximation of the true gradient for problems with dimensions that are powers of two. Theorem 6 proves the optimality of CASG and Proposition 7 provides an efficient construction algorithm.
- We introduce the extended curvature aligned simplex gradient (eCASG) for use in arbitrary dimensions. eCASG heuristically partitions the space and Proposition 16 proves that under this partition eCASG is the optimal simplex gradient based estimator.
- For the construction of our gradient estimators, we introduce a global model framework to estimate any necessary function-dependent information. Instead of requiring further sampling, the framework reuses a history of function evaluations to build a global model which allows us to construct any function-dependent information needed for CASG and eCASG.
- We numerically evaluate our methodology by considering applications in sensitivity analysis and derivative free optimization.
 - Our methodology significantly outperforms or matches the performance of a best-case forward difference estimator which is given all required function-dependent information. As current gradient estimators with $d + 1$ -function evaluations are upper-bounded by the performance of this best-case FD estimator, our proposed method can be used to significantly improve on such methods.
 - Our methodology often matches the performance of central differences, generally considered a far superior gradient estimator but requiring twice the number of function evaluations per gradient estimate. This finding implies that in many situations we can replace central difference methods with our methodology with limited loss in performance while reducing the function evaluations by a factor of two.

1.3. Outline. Section 2 introduces the relevant concepts. In Section 3 we motivate and derive a Taylor-expansion based objective function for the optimization problem related to finding the optimal sampling set for the simplex gradient and derive some crucial simplifications. In Section 4 we present the main results and provide the proof and algorithms for CASG. We additionally provide some intuition behind CASG and an initial comparison to forward differences. In Section 5 we then present the extended curvature aligned simplex gradient. We provide the global model framework algorithm and the empirical results in Section 6. In Section 6 we also discuss in further detail the use of the global model as a separate gradient estimation method. We also consider the cost of the global model framework when no history of function evaluation is available.

1.4. Notation. $\|\cdot\|_2$ is the L_2 norm and $\|\cdot\|_F$ the Frobenius norm. $\text{tr}(\cdot)$ is the trace operator. The general linear group of degree d is GL_d and represents the space of all invertible $d \times d$ -matrices. Given a vector $v \in \mathbb{R}^d$, $\text{diag}(v) \in \mathbb{R}^{d \times d}$ is the diagonal matrix with v along the diagonal. $v \succ 0$ denotes all entries greater than zero and $v \succeq 0$ greater or equal to zero. Given a matrix $B \in \mathbb{R}^{d \times d}$, $\text{diag}(B) \in \mathbb{R}^d$ is the diagonal of the matrix B . $B \succ 0$ denotes B positive definite and $B \succeq 0$ positive semi-definite. \mathbb{R}_+ is the set of all strictly positive real values and \mathbb{Z}_+ is the space of all positive integers. Given a set A , $\mathcal{P}(A)$ is the power-set of A and $|A|$ the size of A . When clear from context, H denotes the second derivative, i.e., the Hessian, of a function. Let the eigen-decomposition be given by $H = RDR^T$, with R orthogonal and D diagonal. By nomenclature we use curvature to refer to the second order behavior of a function.

To disambiguate between different Big-O notations, we use \mathcal{O} for runtime and O for bounding error terms from Taylor's-Theorem. The Hadamard matrix M_k is an orthogonal matrix with the property $(M_k)_{ij}^2 = \frac{1}{d}$ and all positive entries in the k th column.

2. PROBLEM STATEMENT AND SET-UP

The goal is to find the gradient of a differentiable function $f : \mathcal{D} \rightarrow \mathbb{R}$ where $\mathcal{D} \subset \mathbb{R}^d$ has a non-empty interior, while only having access to a noisy black-box. Since function evaluations may be expensive, the function can only be evaluated $d + 1$ times per gradient estimation. The metric by which the quality of the gradient is assessed is the mean squared error (MSE).

2.1. Black Box Evaluation and History. We define the black-box function as a random process to formalize the notion of sequentially evaluating a black-box. The black-box function is given by $\tilde{f} : \mathcal{D} \times \mathbb{Z}_+$ where

$$\tilde{f}(x; i) = f(x) + \epsilon(i).$$

When clear from context, we refer to the black-box function as $\tilde{f}(x)$ and the noise as $\epsilon(x)$. We also define the *evaluation history* as the set

$$\mathcal{E}(I) = \{(x(i), \tilde{f}(x(i); i))\}_{1 \leq i \leq I}.$$

We write $x(i)$ to make it explicit that the choice of where x is evaluated at the i th time-step may depend on the past.

We now introduce the following assumption on the noise.

Assumption 1. $\epsilon(i)$ is assumed to have zero mean and constant and bounded second moment. We additionally we assume that for $i \neq j$, $\epsilon(i)$ is independent of $\epsilon(j)$ and that $x(i)$ is independent of $\epsilon(i)$.

The assumption of zero mean noise and constant and bounded second moment are common in the literature. We additionally make an implicit assumption explicit, namely that subsequent function evaluations have independent noise. The last assumption that $\epsilon(i)$ is independent of $x(i)$ makes explicit that we can not choose x by predicting the noise.

2.2. The Simplex Gradient. The simplex gradient set-up and relevant terminology is in line with other works [31, 41]. Let x' be the point at which we want to estimate the gradient. We define the **sample set** as an ordered set $\mathcal{X} = \{x_i\}_{0 \leq i \leq d}$, with $x_0 = x'$. The **function vector** is the random vector $\tilde{\mathbf{f}}(\mathcal{X})$ such that $\tilde{\mathbf{f}}(\mathcal{X})_i = \tilde{f}(x_i)$. The **difference matrix** $S(\mathcal{X}) \in \mathbb{R}^{d \times d}$ is defined as $S_{ij} = (x_j - x_0)_i$. We will often just refer to it as S when clear from context. We refer to the columns as the **difference vectors** and write $s_i = x_j - x_0$. Lastly, we define the **function difference vector** as $\delta\tilde{\mathbf{f}}(\mathcal{X}) = \tilde{\mathbf{f}}(x_i) - \tilde{\mathbf{f}}(x_0)$.

Lemma 1. Let \mathcal{X} be a sample set such that the size is $d + 1$, $x_0 = x'$ and $\text{span}(S(\mathcal{X})) = \mathbb{R}^d$. Then the unique affine function that interpolates the set of points $\{(x_i, \tilde{f}(x_i))\}_{0 \leq i \leq d}$ is given by

$$\eta^*(x) = \tilde{\mathbf{f}}(x_0) + (\nabla_S \tilde{f}(x_0))^T (x - x_0)$$

where $\nabla_S \tilde{f}(x_0)$ is the **simplex gradient** and is given by

$$\nabla_S \tilde{f}(x_0) = S^{-T} \delta\tilde{\mathbf{f}}$$

with $S^{-T} = (S^T)^{-1}$.

Remark 1. *The simplex gradient is a random variable as it depends on \tilde{f} . Therefore, the mean squared error of the gradient estimator is taken with respect to the probability space $(\Sigma, \mathcal{F}, \mathbb{P})$.*

Forward differences can be seen as an instance of the simplex gradient where the sample set is given by $\{x'\} \cup \{h_i e_i\}_{1 \leq i \leq d}$. Central difference can also be seen as an instance of an over-determined simplex gradient [31].

3. OPTIMIZATION PROBLEM FOR OPTIMAL SAMPLE SET

In this section we motivate and define the objective function which is used to assess the goodness of a sample set for numerical differentiation under the simplex gradient. The objective function is based on the mean squared error and is derived via a Taylor-expansion argument as is common for finite difference schemes [14].

To better understand the mean squared error, we consider its decomposition into the approximation and noise error via the following Proposition.

Proposition 2 (MSE Decomposition). *Let the sample set \mathcal{X} and the black-box function \tilde{f} be given and given Assumption 1 on the noise. Let S be the difference set corresponding to the sample set. Then the mean squared error is given by*

$$\begin{aligned} & \mathbb{E}[\|\nabla_S \tilde{f}(x_0) - \nabla f(x_0)\|_2^2] \\ &= \underbrace{\|\nabla_S f(x_0) - \nabla f(x_0)\|_2^2}_{\text{Approximation Error}} + \underbrace{\sigma^2 \|S^{-1}\|_F^2 + \sigma^2 \|S^{-T} \mathbf{1}\|_2^2}_{\text{Noise Error}}. \end{aligned}$$

Proof. We expand the means squared error after which we proceed term by term

$$\begin{aligned} \mathbb{E}[\|\nabla_S \tilde{f}(x_0) - \nabla f(x_0)\|_2^2] &= \mathbb{E}[\|\nabla_S \tilde{f}(x_0) - \nabla_S f(x_0) + \nabla_S f(x_0) - \nabla f(x_0)\|_2^2] \\ &= \mathbb{E}[\|\nabla_S \tilde{f}(x_0) - \nabla_S f(x_0)\|_2^2] + \|\nabla_S f(x_0) - \nabla f(x_0)\|_2^2 \\ &\quad + 2\mathbb{E}[\left(\nabla_S \tilde{f}(x_0) - \nabla_S f(x_0)\right)^T \left(\nabla_S f(x_0) - \nabla f(x_0)\right)]. \end{aligned}$$

By linearity of the simplex gradient we have that $\mathbb{E}[\|\nabla_S \tilde{f}(x_0) - \nabla_S f(x_0)\|_2^2] = \mathbb{E}[\|\nabla_S \epsilon(0)\|_2^2]$ where we write $\nabla_S \epsilon(0) = S^{-T} \delta \epsilon(\mathcal{X})$ with $\delta \epsilon(\mathcal{X}) = [\epsilon(1) - \epsilon(0), \dots, \epsilon(d) - \epsilon(0)]^T$. We then have for the first term

$$\begin{aligned} \mathbb{E}[\|\nabla_S \epsilon\|_2^2] &= \mathbb{E}[\delta \epsilon(\mathcal{X})^T S^{-1} S^{-T} \delta \epsilon(\mathcal{X})] \\ &= \text{tr}(S^{-1} S^{-T} (\sigma^2 I + \sigma^2 \mathbf{1}\mathbf{1}^T)) \\ &= \sigma^2 \|S^{-T}\|_F^2 + \sigma^2 \|S^{-T} \mathbf{1}\|_2^2. \end{aligned}$$

where we used the result from [34] that for any random vector \mathbf{X} , with mean μ and covariance matrix Σ , and symmetric matrix A we have $\mathbb{E}[\mathbf{X}^T A \mathbf{X}] = \mu^T A \mu + \text{tr}(A \Sigma)$. The second term $\|\nabla_S f(x_0) - \nabla f(x_0)\|_2^2$ is already in the correct form. Lastly, the cross term $\mathbb{E}[\left(\nabla_S \tilde{f}(x_0) - \nabla_S f(x_0)\right)^T \left(\nabla_S f(x_0) - \nabla f(x_0)\right)]$ is easily seen to equal zero since $\mathbb{E}[\nabla_S \tilde{f}(x_0)] = \nabla_S f(x_0)$. \square

While the noise error only depends on the noise level and distribution of points, the approximation error also depends on the function structure. Since we do not have access to the true function f , we need use some approximation of f . However, even with an approximation of f , the MSE may be difficult to minimize directly. Instead, we introduce a bound on the approximation error.

3.1. Approximation Error Bound. While there exist multiple methods by which to estimate the approximation error, we proceed via a Taylor argument as done in many other works [32, 14, 13]. The crucial difference is that previous works upper bound the second order term, while we retain the second order term exactly and only bound the higher order terms.

Lemma 3. *Let $f \in \mathcal{C}^2$ and let $\|S\|_2 \leq h$ for some $h \in \mathbb{R}_+$. Then we have*

$$\|\nabla_S f(x_0) - \nabla f(x_0)\|_2^2 = \frac{1}{4} \|S^{-T} [s_1^T \nabla^2 f(x_0) s_1, \dots, s_d^T \nabla^2 f(x_0) s_d]^T\|_2^2 + O(h^3).$$

The proof is in Appendix A.1 and is a simple application of Taylor's Theorem.

3.2. Objective Function. When using the bound on the approximation error and the noise error, the only variables are the noise level σ , the given Hessian matrix H , and the sample difference set S . To control the error due to higher-order effects, the hyperparameter h is introduced. The optimization problem is then given by the following.

Definition 4. *Let $H \in \mathbb{R}^{d \times d}$ be symmetric, $\sigma \in \mathbb{R}_+$ and $h \in \mathbb{R}_+$. Let*

$$\mathbf{AE} = \frac{1}{4} \|S^{-T} [s_1^T H s_1, \dots, s_d^T H s_d]^T\|_2^2$$

be the approximation error and

$$\mathbf{NE} = \sigma^2 \|S^{-1}\|_2^2 + \sigma^2 \|S^{-T} \mathbf{1}\|_2^2$$

be the noise error. We then define the function $l_{H,\sigma,h} : \mathbb{R}^{d \times d} \rightarrow [0, \infty]$ as

$$l_{H,\sigma,h}(S) = \begin{cases} \mathbf{AE} + \mathbf{NE} & \text{if } h \geq \|S\|_2 \text{ and } S \in GL_d \\ \infty & \text{, else.} \end{cases}$$

and its reparametrization in SVD form

$$l_{H,\sigma,h}(U, \Sigma, V) = \begin{cases} l_{H,\sigma,h}(U \Sigma V^T) & \text{if } U, V \text{ orthogonal, } D \text{ diagonal, and } D \succeq 0. \\ \infty & \text{, else.} \end{cases}$$

When clear from context, we drop the H, σ, h subscript and write $l(S)$ or $l(U, \Sigma, V)$.

Remark 2. *Defining the objective function on the extended real number line and setting it to infinity outside of the valid input makes the optimization problem well defined. Specifically, a minimizer exists as the objective function is continuous and defined on a compact domain.*

The following Proposition significantly simplifies the objective function and allows us solve the optimization problem in the basis in which H is diagonal.

Proposition 5. *Let H be a symmetric matrix and let R be an orthogonal matrix such that $R^T H R = D$. Defining $S' = R^T S$ then $l_{H,\sigma}(S) = l_{D,\sigma}(S')$. Furthermore, $l_{D,\sigma}(S) = l_{-D,\sigma}(S)$.*

Proof. Note that $\|S^{-1}\|_F = \text{tr}(R^T S'^{-T} S'^{-1} R)$ and by the cyclic property of trace $\|S^{-1}\|_F = \|S'^{-1}\|_F$. Furthermore, since orthogonal operations do not change norms $\|S^{-T} \mathbf{1}\|_2^2 = \|S'^{-T} \mathbf{1}\|_2^2$. For the approximation error note that $s_i^T H s_i = s_i'^T D s_i'$. As established, orthogonal matrices do not change norms and hence $\|S^{-T} [s_1^T D s_1, \dots, s_d^T D s_d]^T\|_2^2 = \|S'^{-T} [s_1'^T D s_1', \dots, s_d'^T D s_d']^T\|_2^2$. The invariance to negating the diagonal is due to the absolute homogeneity property of the norm. \square

While more manageable, the objective function is not trivial to minimize due its remaining non-convexity and non-linearity. This is unlike standard forward difference where the difference matrix has orthogonal columns which allows the optimization problem to separate into a sum of one-dimensional convex functions which are easy to solve.

4. CURVATURE ALIGNED SIMPLEX GRADIENT

We now present the results and methods to compute

$$S^* = \arg \min_{S \in \mathbb{R}^{d \times d}} l_{H,\sigma,h}(S)$$

where $l_{H,\sigma,h}(S)$ is given in Definition 4. We call the simplex gradient which uses S^* the *Curvature Aligned Simplex Gradient* (CASG), since our method naturally aligns difference vectors along directions of low curvature.

The results will be purely theoretical, as we assume a Hessian H and noise-level σ to be given. In Section 6 we show how to construct CASG for real-world applications using our global model framework. We make this precise with the following assumption on the parameters.

Assumption 2. *The matrix $H \in \mathbb{R}^{d \times d}$ is symmetric, and $\sigma, h \in \mathbb{R}_+$.*

Recall that for symmetric matrices we may write $H = RDR^T$ with orthogonal matrix R and diagonal matrix D . To simplify the presentation of the problem, we use Proposition 5 and general properties of diagonalizable matrices to make the following assumption on H and D without any loss of generality.

Assumption 3. *H has positive trace and D is in increasing order.*

We now introduce the final assumption we will be using.

Assumption 4. *The dimension of the problem is a power of two.*

While Assumption 4 may seem artificial, it appears naturally when deriving the analytic solution. We discuss in Section 5 how to generalize the results from this section to arbitrary dimensions.

We now present the results used to construct a minimizer S^* .

Theorem 6. *Assume that for parameters H, σ and h Assumptions 2-4 hold and recall the eigen-decomposition $H = RDR^T$. The global minimum of $l_{H,\sigma,h}$, S^* , is given by $RU^*\Sigma^*(V^*)^T$ where*

- $U^* = I$
- Σ^* is the solution to the following optimization problem

$$\Sigma^* = \arg \min_{\Sigma} \begin{cases} \frac{(\sum_{i=1}^d D_i \Sigma_i^2)^2}{4d \Sigma_{max}^2} + \sigma^2 \sum_{i=0}^d \frac{1}{\Sigma_i^2} + \sigma^2 \frac{1}{\Sigma_{max}^2} d & \text{if } hI \succeq \Sigma \succ 0 \\ \infty & \text{otherwise.} \end{cases}$$
- $V^* = M_k$ where $k = \arg \max_k \Sigma_k$. Recall that M_k is the Hadamard matrix with the entries of the k th row being $1/\sqrt{d}$.

The optimization problem for Σ^* can be solved without the need of numerical methods. Algorithm 2 provides the construction of Σ^* .

Proposition 7. *The optimization problem for Σ^* as given in Theorem 6 is well defined, has a unique solution and can be computed in $\mathcal{O}(d)$ time.*

4.1. Algorithm and Runtime. Algorithm 1 describes the procedure to construct the minimizer of the objective function where the problem follows Assumptions 2 and 4. The first six lines transform the input to align with Assumption 3. By Theorem 6 we have that $U^* = I$ leaving only the computation of Σ^* and V^* . We obtain Σ^* via the function call $\text{Get}\Sigma^*(D, \sigma, h)$, given

Algorithm 1 CASG

```

1: procedure COMPUTE  $S^*(H, \sigma, h)$ 
2:    $d \leftarrow$  Dimension of  $H$ 
3:    $R, D \leftarrow$  Diagonalize  $H$ ;  $D$  a vector sorted in increasing order
4:   if  $\sum_{i=1}^d D_i < 0$  then
5:     return Compute  $S^*(-H, \sigma, h)$  ▷ Call function with negated Hessian.
6:   end if
7:    $\Sigma^* \leftarrow$  Get $\Sigma^*(D, \sigma, h)$  ▷ In descending order.
8:    $V^* \leftarrow$  Hadamard matrix with first row all ones
9:    $S_D^* \leftarrow \Sigma^*(V^*)^T$ 
10:  return  $RS_D^*$ 
11: end procedure

```

by Algorithm 2, to obtain Σ^* . To transform the solution to the original space of H we use Proposition 5 to perform a change of basis on S_D^* which yields S^* .

The runtime of this algorithm is dominated by the eigendecomposition of H , which has runtime $\mathcal{O}(d^3)$. The computation of Σ^* is done in linear time by Proposition 7. The Hadamard matrix is computed via the Sylvester’s Construction which has runtime $\mathcal{O}(d^2)$.

While the runtime of CASG is larger than the linear runtime of many finite difference methods, we note that for numerical differentiation the assumption is that function evaluations are expensive. Hence, we trade computational speed for accuracy in gradient estimates and hence fewer function evaluations.

4.2. Intuition and Initial Numerics. We now present some initial numerics to demonstrate the benefit of CASG compared to forward differences on a toy example. To compare the methods, we estimate the gradient at the origin of a quadratic function corrupted by additive noise. Specifically, we consider the function $\tilde{f}_k(x, y) = kx^2 + y^2 + \epsilon$, where $k \in \mathbb{R}$ is used to control the conditioning of the Hessian and $\epsilon \sim \mathcal{N}(0, 0.01^2)$. We provide the exact Hessian and noise level to both CASG and FD. The mean squared error is then exactly given by the objective value.

To obtain the error bars for the mean squared error plots in Figures 1b and 1e we perform 1,000 gradient estimates to then plot the 25th and 75th percentile values. The contour lines of the quadratic form given by the Hessian of the noiseless quadratic are depicted in Figures 1a and 1d and represent the error of a directional gradient estimate using finite differences. In Figures 1c and 1f we plot the average of the lengths of the two difference vectors.

When the Hessian is positive definite, we see in Figure 1a that CASG aligns the difference vectors along low curvature directions to achieve an approximation error comparable to FD while increasing the difference vector length to decrease the noise error. We confirm that this happens consistently for H ’s with different condition numbers in Figure 1c. The overall improvement is apparent in Figure 1b where the mean squared error is magnitudes lower whenever the Hessian is ill-conditioned and the method can exploit low curvature directions.

When the Hessian is indefinite, in addition to exploiting low curvature directions we observe that when aligning the difference vectors close to the zero-set lines, as seen in Figure 1d, the approximation error is close to zero. Increasing the length of the difference vectors will then decrease the noise error without increasing the approximation error drastically. In Figure 1e we see that the mean squared error is lowest when $k = -1$, which happens when the difference vectors are fully aligned with the zero-set lines. This is because there is no approximation error

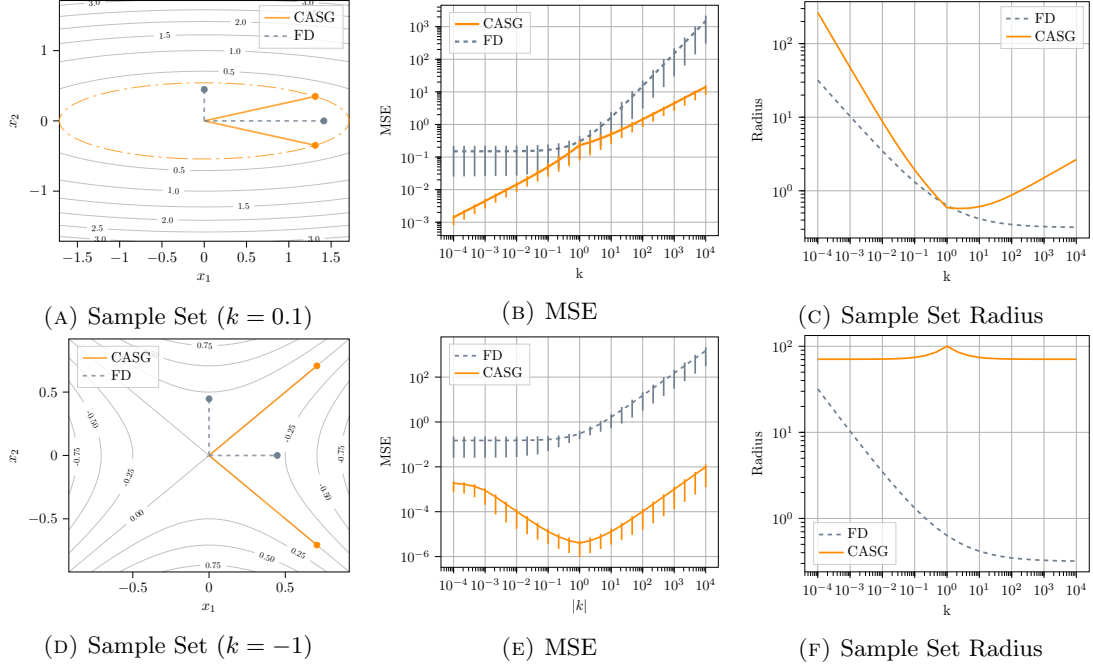


FIGURE 1. Comparing forward differences (FD) with optimal difference vector lengths [14] to the curvature aligned simplex gradient (CASG). The first row corresponds to a positive definite Hessian with $k \in [10^{-4}, 10^4]$. The bottom row represents an indefinite Hessian with $k \in [-10^4, -10^{-4}]$ and with $h = 10^2$.

and the orthogonal layout of the difference vectors is optimal for the noise error. In the case $k = -1$, CASG also has the same performance as central differences, as neither will suffer from the approximation error.

4.3. Proof of Theorem 6. By Proposition 5, it suffices to rotate a minimizer of $l_{D,\sigma,h}$ by R to obtain a minimizer for $l_{H,\sigma,h}$. It remains to prove the result for diagonal matrices D .

For the proof of Theorem 6 we need the following Propositions. We defer the proof of those to Appendix A.2. For the following results let Assumptions 2-4 hold.

Proposition 8. For a diagonal matrix $D \in \mathbb{R}^{d \times d}$ and positive real numbers $\sigma, h \in \mathbb{R}_+$ define the function

$$(4.1) \quad l_{D,\sigma,h}(U, \Sigma) = \begin{cases} \frac{a_{D,\sigma}(U, \Sigma)^2}{4d\Sigma_{max}^2} + \sigma^2 \sum_{i=1}^d \frac{1}{\Sigma_i^2} + \sigma^2 \frac{d}{\Sigma_{max}^2} & \text{if } hI \succeq \Sigma \succ 0 \\ \infty & \text{otherwise,} \end{cases}$$

with orthogonal $U \in \mathbb{R}^{d \times d}$, diagonal $\Sigma \in \mathbb{R}^{d \times d}$, and $a_{D,\sigma}(U, \Sigma) = \text{tr}(\Sigma U^T D U \Sigma)$. Then we have

$$l_{D,\sigma,h}(U, \Sigma) \leq \min_V l_{D,\sigma,h}(U, \Sigma, V).$$

Proposition 9. The global minimizers U' and Σ' of $l_{D,\sigma,h}(U, \Sigma)$ are given by U' being the identity matrix and Σ' being the solution to $\min_S l_{D,\sigma,h}(I, S)$. The minimization problem for S' is equivalent to the one given in Theorem 6.

Proposition 10. *Let U' and Σ' be the minimizers of $l_{D,\sigma,h}(U, \Sigma)$. Letting V' be the Hadamard matrix M_k , where $k = \arg \max_i \Sigma_i$, we have that $l_{D,\sigma,h}(U', \Sigma') = l_{D,\sigma,h}(U', \Sigma', V')$.*

Proof. [Proof of Theorem 6] Notice that U', Σ' given by Proposition 9 and V' given by Proposition 10 have the same form as U^*, Σ^* and V^* in Theorem 6. Hence, it remains to show that they are in fact the global minimizers of $l_{D,\sigma,h}$. Consider the following chain of inequalities.

$$\begin{aligned} l_{D,\sigma,h}(U', \Sigma', V') &\geq l_{D,\sigma,h}(U^*, \Sigma^*, V^*) \\ &= \min_{U, \Sigma} \min_V l_{D,\sigma,h}(U, \Sigma, V) \\ &\geq \min_{U, \Sigma} l_{D,\sigma,h}(U, \Sigma) \quad \text{by Proposition 8} \\ &= l_{D,\sigma,h}(U', \Sigma'). \end{aligned}$$

Due to Proposition 10 we know $l_{D,\sigma,h}(U', \Sigma', V') = l_{D,\sigma,h}(U', \Sigma')$. Hence the above chain of inequalities becomes a chain of equalities and specifically $l_{D,\sigma,h}(U', \Sigma', V') = l_{D,\sigma,h}(U^*, \Sigma^*, V^*)$. Hence U', Σ' and V' are also the global minimizers of $l_{D,\sigma,h}$. Rotating the result by R completes the proof and provides a minimizer of $l_{H,\sigma,h}$. \square

4.4. Proof of Proposition 7. We now prove Proposition 7 and Algorithm 2 which computes a global minimizer Σ^* . To keep notation tight, we let $\lambda \in \mathbb{R}^d$ represent the diagonal of the square of Σ , i.e. $\lambda = \text{diag}(\Sigma^2)$.

To develop an efficient method to solve for a global minimum we note the following useful properties.

Proposition 11. *λ^* is in decreasing order, i.e. $\lambda_i^* \leq \lambda_j^*$ whenever $i \leq j$. Furthermore, $\lambda_i^* = h^2$ for all $1 \leq i \leq d$ such that $D_i \leq 0$.*

The proof is in Appendix A.3.1.

Remark 3. *Due to λ^* being in decreasing order, we know that $\lambda_{max}^* = \lambda_1^*$ which will allow us to avoid any issues of non-differentiability of the maximum operator.*

We now proceed by presenting a closed-form solution for λ^* with known run-time.

4.4.1. Finding all Candidate Solutions. We solve the optimization problem by constructing a set of candidate solutions. The candidate solutions compromise the extrema of a set of unconstrained problems which we can solve analytically. We now formalize this. All proofs for this section are in Appendix A.3.2.

Let $A \in \mathcal{P}(\{1, \dots, d\})$ be an **active set**. A will contain all the indices of λ which will be set to h^2 . We then write the

$$\lambda_i^{(A)} = \begin{cases} h^2 & \text{if } i \in A, \\ \lambda_i & \text{otherwise.} \end{cases}$$

Using Proposition 11 to replace λ_{max} with λ_1 we let the unconstrained function $l_{D,\sigma,h,A} : \mathbb{R}_+^d \rightarrow \mathbb{R}$ be

$$l_{D,\sigma,h,A}(\lambda) := \frac{(\sum_{i=1}^d D_i \lambda_i^{(A)})^2}{4d\lambda_1^{(A)}} + \sigma^2 \sum_{i=0}^d \frac{1}{\lambda_i^{(A)}} + \sigma^2 \frac{1}{\lambda_1^{(A)}} d.$$

We write $l_A(\lambda)$ instead of $l_{D,\sigma,h,A}(\lambda)$ when clear from context.

Since the function l_A is differentiable on its domain, the stationary points are well defined. We denote the set of stationary points associated with the active set A by $\lambda_A^* = \{\lambda^{(A)} : \nabla l_A(\lambda) = 0\}$.

We now show that given the above reformulation there exists an active set A such that the global solution λ^* is contained in λ_A^* . Additionally, instead of computing solutions for 2^d possible active sets, we need to check at most d active sets due to Proposition 11.

Proposition 12. *Let $K = \{i | D_i \leq 0\}$ and $A_J = \{1, \dots, J\}$. Then there exists $J \in \{|K|, \dots, d\}$ such that $\lambda^* \in \lambda_{A_J}^*$.*

We now need to show that finding λ_A^* can be done efficiently. For this we first present the following.

Proposition 13. *Let $K = \{i | D_i \leq 0\}$ and A be some active set such that $K \subseteq A$. Then the set λ_A^* consists of all λ which satisfy*

$$\begin{aligned} \lambda_1 &= \begin{cases} h^2 & \text{if } 1 \in A, \\ \frac{2d}{aD_1} \left(\frac{a^2}{4d} + \sigma^2(d+1) \right) & \text{otherwise;} \end{cases} \\ \lambda_i &= \begin{cases} h^2 & \text{if } i \in A, \\ \sigma \sqrt{\frac{2d\lambda_1}{aD_j}} & \text{otherwise,} \end{cases} & \text{for } 2 \leq i \leq d, \\ a &= \sum_{i \notin A} D_i \lambda_i + h^2 \sum_{i \in A} D_i. \end{aligned}$$

We now present the unique solution for a for a given active set, which then allows us to immediately compute the unique candidate solution given by Proposition 13.

Proposition 14. *Let $K = \{i | D_i \leq 0\}$ and $A_J = \{1, \dots, J\}$. Then the a which satisfies the equations given in Proposition 13 is unique and is given by*

- If A_J is empty, then we have

$$a = \sqrt{2} \left(\frac{d\sigma^2}{D_1} \left(C \sqrt{8D_1(d+1) + C^2} + 2D_1(d+1) + C^2 \right) \right)^{1/2}$$

$$\text{with } C = \sum_{i=2}^d \sqrt{D_i};$$

- Otherwise,

$$a = \begin{cases} \frac{\sqrt[3]{\frac{2}{3}c_2}}{\sqrt[3]{\sqrt{3}\sqrt{27c_1^2 - 4c_2^3} + 9c_1}} + \frac{\sqrt[3]{\sqrt{3}\sqrt{27c_1^2 - 4c_2^3} + 9c_1}}{\sqrt[3]{18}} & \text{if } 27c_1^2 - 4c_2^3 \geq 0, \\ \cos(\theta/3) 2\sqrt{\frac{c_2}{3}} & \text{otherwise,} \end{cases}$$

$$\text{where } c_1 = \sigma \sqrt{\frac{dh^2}{2}} \sum_{i=J+1}^d \sqrt{D_i}, c_2 = \sum_{i=1}^J D_i h^2 \text{ and } \theta = \arccos\left(\frac{9c_1}{\sqrt{12c_2^3}}\right).$$

4.4.2. *Constructing λ^* in Linear Runtime.* While Propositions 13 and 14 tell us how to construct solutions for an active set, it remains to select the global minimum of all possible solutions. The naive implementation of finding λ^* has runtime $\mathcal{O}(d^2)$, since there are d active sets to consider by Proposition 12 and constructing λ_A^* for each A is also of linear runtime. We can improve the runtime to be linear. While this will not improve the theoretical runtime of the method, in practice we have seen it be helpful.

To construct λ^* in linear time, we observe the following proposition. The Algorithm 2 then uses the result as given by Algorithm 3 to compute λ^* in linear time. Since by Proposition 13 and 14 the candidate solution for an active set is unique, we let λ_A^* represent the solution rather than the solution set.

Algorithm 2 Get Σ^*

```

1: procedure GET $\Sigma^*(D, \sigma, h)$ 
2:    $d \leftarrow$  Dimension of  $D$ 
3:   if  $\sum_{i=1}^d D_i = 0$  then
4:     return  $h$ 
5:   end if
6:    $J \leftarrow |\{i | D_i \leq 0, 1 \leq i \leq d\}|$ 
7:    $c_1, c_2 \leftarrow \sum_{i=J+1}^d \sqrt{D_i}, \sum_{i=1}^J D_i$ 
8:   while True do
9:      $\lambda_{J+1}, a \leftarrow$  Get $\lambda_{J+1}(J, D, \sigma, h, c_1, c_2)$ 
10:     $c_1, c_2 \leftarrow c_1 - \sqrt{D_{J+1}}, c_2 + D_{J+1}$ 
11:    if  $\lambda_{J+1} \leq h^2$  and  $J < d$  then
12:      break
13:    end if
14:     $J \leftarrow J + 1$ 
15:  end while
16:   $\lambda_i \leftarrow h^2$  ▷ For  $1 \leq i \leq J$ .
17:   $\lambda_j \leftarrow \sigma \sqrt{\frac{2dh^2}{aD_j}}$  ▷ For  $J + 1 \leq j \leq d$ .
18:  return  $\sqrt{\lambda}$ 
19: end procedure

```

Proposition 15. *Let $K = \{i | D_i \leq 0\}$ and J be the smallest integer in the set $\{|K|, \dots, d\}$ such that $\lambda_{A_J}^*$ satisfies all constraints, i.e. $h^2 \succeq \lambda_{A_J}^*$. Then it follows that $l(\lambda^*) = l(\lambda_{A_J}^*)$. Additionally, if $J \geq 1$ the comparison $h^2 \succeq \lambda_{A_J}^*$ can be done in constant time.*

The proof is in Appendix A.3.3.

5. EXTENDED CURVATURE ALIGNED SIMPLEX GRADIENT (ECASG)

Theorem 6 only applies for dimensions which are powers of two. Hence, we introduce a heuristic method which subdivides the full space such that we can use CASG via Theorem 6. First we describe how to partition the subspace and how that may lead to a useful decomposition of the objective function. We then describe a method by which to choose the partition such that we can exploit the results for spaces with dimensions of powers of two and which aligns with the intuition developed in Section 4.2.

Partition Set-up. Let $\{B_i\}_{1 \leq i \leq k}$ be a partition of the standard basis $\{e_i\}_{1 \leq i \leq d}$ into k sets, with each B_i being a cell of the partition represented as a matrix. We let B be the concatenation of the cells, $B = [B_1 \ B_2 \ \dots \ B_k]$. Since B is simply a reordering of the standard basis, the matrix is orthogonal. Using this partition, we enforce that each difference vector is spanned by one of the cells. We can now write $S = BS_B$, where the i th columns of S_B are the coefficients of the difference vector s_i in the B_i basis. It follows that S_B is a block-diagonal matrix, with the i th block representing the coefficients of the differences vectors spanned by cell B_i . It immediately follows that, if it exists, the matrix S_B^{-1} is also a block diagonal matrix, with the i th block of S_B^{-1} being equal to $S_{B_i}^{-1}$.

Algorithm 3 Get λ_{J+1}

```

1: procedure GET $\lambda_{J+1}(J, D, \sigma, h, c_1, c_2)$ 
2:    $d \leftarrow$  Dimension of  $D$ 
3:   if  $J = 0$  then
4:      $J \leftarrow c_1 - \sqrt{D_1}$ 
5:      $a \leftarrow \sqrt{2} \left( \frac{d\sigma^2}{D_1} (J \sqrt{8D_1(d+1) + J^2} + 2D_1(d+1) + J^2) \right)^{1/2}$ 
6:      $\lambda_1 \leftarrow \frac{2d}{aD_1} \left( \frac{a^2}{4d} + \sigma^2(d+1) \right)$ 
7:   else
8:      $c_1, c_2 \leftarrow \sigma \sqrt{\frac{dh^2}{2}} c_1, h^2 c_2$ 
9:      $disc \leftarrow 81c_1^2 - 12c_2^3$ 
10:    if  $disc < 0$  then
11:       $\theta \leftarrow \cos^{-1} \left( 9 \frac{c_1}{\sqrt{12c_2^3}} \right)$ 
12:       $a \leftarrow \frac{4}{3} \cos(\theta/3)^2 c_2$ 
13:    else
14:       $a \leftarrow \frac{\sqrt[3]{\frac{2}{3}c_2}}{\sqrt[3]{\sqrt{disc+9c_1}}} + \frac{\sqrt[3]{\sqrt{disc+9c_1}}}{\sqrt[3]{18}}$ 
15:    end if
16:     $\lambda_{J+1} \leftarrow \sigma \sqrt{\frac{2dh^2}{aD_{J+1}}}$ 
17:  end if
18:  return  $\lambda_{J+1}, a$ 
19: end procedure

```

Proposition 16. *Let Assumptions 2 and 3 hold. Given a fixed partition $\{B_i\}_{1 \leq i \leq k}$ and a block-diagonal matrix S_B with S_{B_i} being the i th block providing the coordinates of the difference vectors in space spanned by B_i , we have $l_{D, \sigma, h}(BS_B) = \sum_{i=1}^k l_{D_{B_i}, \sigma, h}(S_{B_i})$ with $D_{B_i} = B_i D B_i^T$.*

Proof. If S_B is not invertible then at least one block will not be invertible and hence the two sides of the equation are trivially equal as they equal ∞ . When S_B is invertible the result follows immediately from the block structure of S_B and orthogonality of B . \square

The Proposition allows us to minimize with respect to the block-diagonal matrix S_B . Letting each cell in the partition have dimension power of two, we can use Theorem 6 to find the optimal solution by applying CASG to each cell. While the minimizer may have a larger function value than minimizing $l_{D, \sigma, h}(S)$ directly, we have empirically found that carefully choosing B leads to good gradient estimates. We now describe our heuristic method of choosing such a partition. **Choosing the Partition.** To use Theorem 6, we enforce that the dimension of the span of each cell be a power of two. We do so by using a binary expansion of the dimension $d = \sum_{i=1}^{\lfloor \log(d) \rfloor} c_i 2^i$, and adding a cell of size 2^i for every $c_i = 1$. It now remains to describe the subspace each cell will span.

As developed in Section 4.2, we use the intuition that when negative and positive curvature directions exist, they are paired together such that CASG can exploit zero-set lines. When only positive or negative curvature regions remain, we pair high with low curvature directions to allow CASG to align the sample set along the low curvature direction.

We describe the full eCASG method in Algorithm 4. Since the Hessian is assumed to be diagonal, the curvature directions, i.e. eigenvectors, are given by the standard basis vectors. We proceed greedily by iterating through the partition cells, B_i , and adding the direction of highest

Algorithm 4 Subdivide Space (eCASG)

```

1: procedure SUBDIVIDE SPACE( $D$ ) ▷  $D$  is sorted in increasing order
2:    $d \leftarrow$  Dimension of  $D$ 
3:    $d_{bin} \leftarrow$  binary coefficients of  $d$  ▷ Least significant digit last
4:    $start, end \leftarrow 0, d$ 
5:    $i \leftarrow d_{bin}.length - 1$  ▷ Cell index starts with most significant digit
6:    $B \leftarrow$  List of cells
7:   while  $start \leq end$  do
8:     if  $d_{bin}[i] = 1$  and cell  $B[i]$  is not full then
9:       if  $i = 0$  then
10:          $B[i].add(D[start])$ 
11:          $start \leftarrow start + 1$ 
12:       else
13:          $B[i].add(D[start])$ 
14:          $B[i].add(D[end])$ 
15:          $start \leftarrow start + 1$ 
16:          $end \leftarrow end - 1$ 
17:       end if
18:     end if
19:      $i \leftarrow (i - 1) \bmod d_{bin}.length$ 
20:   end while
21:   return  $B$ 
22: end procedure

```

curvature and the direction of lowest curvature from the set of possible directions. We then remove these directions from the set of possible directions and move to the next cell and repeat.

6. GLOBAL MODEL FRAMEWORK AND NUMERICAL RESULTS

6.1. Global Model Framework. We now discuss the global model framework for obtaining the Hessian needed for computing CASG. The idea behind the framework is simple. In many applications, the function will be evaluated multiple times in various regions of the domain. While the information we obtain may not be accurate enough for a gradient estimate, it may still be valuable to guide us in selecting the right sample set for a local gradient estimate. In our framework we formalize this via Algorithm 5. For the global model framework several input variables are needed. One is the evaluation history set \mathcal{E} as described in Section 2. Then we need a model space and a model fitting function. We let the fitting function be given by $\Phi(\mathcal{E}) \rightarrow \phi$ which maps evaluation history set to a global model $\phi : \mathbb{R}^d \rightarrow \mathbb{R}$. In many applications we would not like to use the complete evaluation history, as some points may be poorly spread out for the chosen model space and fitting function. Hence, we allow for a filter function on the evaluation history $\mathcal{F}(\mathcal{E}) \rightarrow \mathcal{E}_{\mathcal{F}}$ where $\mathcal{E}_{\mathcal{F}} \subseteq \mathcal{E}$. Lastly, we denote by \mathcal{G} the gradient estimator which maps a Hessian estimate and the current evaluation point to a gradient estimate and also returns the function evaluations which happened as a consequence of estimating the gradient. We return the gradient estimate and the new function evaluation history.

While the framework requires the choice of a model space, fitting function, and an evaluation history filter, such parameters often arise from the application domain as we will see in the following applications.

Algorithm 5 Global Model Framework

```

1: procedure GLOBAL MODEL FRAMEWORK( $\mathcal{E}, \Phi, \mathcal{F}, \mathcal{G}, x_0$ )
2:    $\mathcal{E}_{\mathcal{F}} \leftarrow \mathcal{F}(\mathcal{E})$  ▷ Filter evaluation history
3:    $\phi \leftarrow \Phi(\mathcal{E}_{\mathcal{F}})$  ▷ Fit global model
4:    $H_{global} = \nabla^2 \phi(x_0)$ 
5:    $g, \mathcal{E}_{curr} \leftarrow \mathcal{G}(H_{global}, x_0)$  ▷ Grad estimate
6:    $\mathcal{E} \leftarrow \mathcal{E} \cup \mathcal{E}_{curr}$  return
7:    $g, \mathcal{E}$ 
8: end procedure

```

A natural question is that if the global model is good enough as a Hessian estimator, should it not also be a good gradient estimator. We will empirically demonstrate this to be not true. The intuition is that a gradient estimator is allowed to sample locally, while the global model will generally not have these local evaluations present in the evaluation history and hence be less accurate close to the evaluation point.

6.1.1. *Global Model: Cubic Spline.* For our experiments we found the cubic spline radial basis function to be a good global model. We use the implementation by `scipy` [49] and extend it to allow for the analytic computation of the gradient and Hessian once the model has been fit. When some of the points in the evaluation history are close together, and the fit needs to be regularized, we also used the smoothing parameter that is part of the fitting procedure. We will specify when we use the smoothing parameter.

6.2. **Sensitivity Analysis.** Sensitivity analysis is used to understand how the response of a system depends on small changes in the input. Often this is done by computing the gradient locally [40], which provides an ideal application area under which to assess CASG and eCASG. To replicate a corrupted system, we add additive Gaussian noise of which we assume to know the noise level as is common for assessing gradient estimation methods [44, 4, 12].

We compare our method against forward (FD) and central (CD) differences and the gradient estimate given by the global model, i.e. $\nabla \phi$. For comparison, our method and FD will be given both global model information and exact Hessian information. Forward differences will be used as given in [6]. We use CD where the difference vector lengths are set to the step-size parameter h [14]. This is a fair comparison as CD has no second order error and is used as a best case comparison. For our CASG, eCASG, FD and CD, the step-size hyperparameter h is found by a hyperparameter search. The global model gradient estimate is attained by simply differentiating the global model.

To assess the goodness of the gradient estimate by our method, FD and CD, we use the exact version of the mean squared error as given in Proposition 2. While Proposition 2 is stated only for the standard simplex gradient, it can be immediately extended for central differences. The gradient estimate from the global method is assessed by considering the squared norm of the difference to the true gradient. For the global model there is no noise component as the randomness is only due to the function evaluation history, which we assume to be given for any local gradient estimate.

The main results are given in Figures 2 and 4. For Figures 2a, 2b, 4a and 4b we chose 100 points uniformly at random from the domain and for each gradient estimation method computed the log ratio as in [37] between the respective method and the given version of CASG, i.e. $\log_2\left(\frac{MSE_{method}}{MSE_{CASG}}\right)$.

To make the cost of using a function evaluation history more explicit we also plot the error of each method against the number of points in \mathcal{E} . Specifically, for Figures 2c and 4c the global method was fitted with a variable number of points as given by the x-axis. The error-bars represent the 25th and 75th percentile of the MSE values at the 100 randomly chosen points, with the line being the median.

For the global model we use no-smoothing, as the function evaluation points will be sufficiently spread out to mitigate the effect of noise.

6.2.1. *Ackley function.* The Ackley function is a common test function due to its high degree of non-linearity and is given by $x_i \in [-0.5, 0.5]$

$$f(x_0 \cdots x_n) = -20 \exp\left(-0.2 \sqrt{\frac{1}{n} \sum_{i=1}^n x_i^2}\right) - \exp\left(\frac{1}{n} \sum_{i=1}^n \cos(2\pi x_i)\right) + 20 + e.$$

For the experiment we set the dimension to 8 and the noise level to $\sigma = 10^{-5}$. The set of step-sizes we consider as hyperparameter is $\{0.1, 0.05, 0.01\}$. For the RBF we sample 10^4 points for the global model for the box plots. Since the dimension is 8 we can use CASG directly.

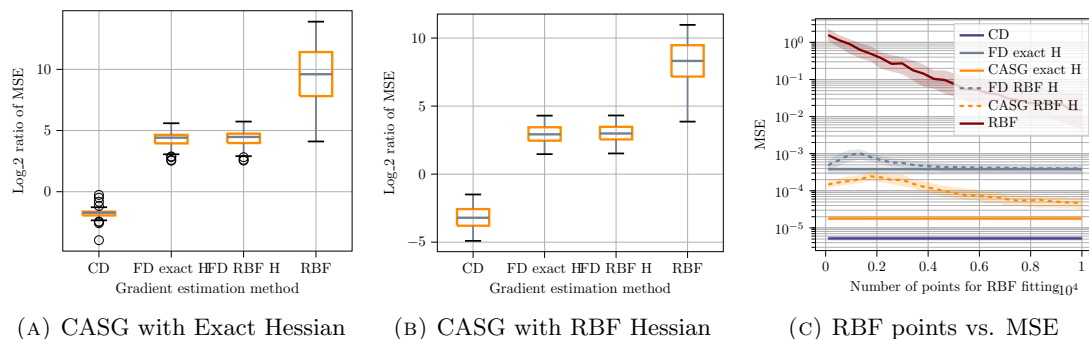


FIGURE 2. Comparison of gradient estimation methods for Ackley with $d = 8$ and $\sigma = 10^{-5}$.

6.2.2. *ODE Model: Cell differentiation in the colon.* We consider a model for cell differentiation in the colon which has been used for sensitivity analysis [40, 33]. The process tracks three variables and is given by the following dynamics

$$\begin{aligned} \frac{dN_0}{dt} &= (\alpha_3 - \alpha_1 - \alpha_2)N_0 - \frac{k_0 N_0^2}{1 + m_0 N_0} \\ \frac{dN_1}{dt} &= (\beta_3 - \beta_1 - \beta_2)N_1 + \alpha_2 N_0 - \frac{c_1 N_1^2}{1 + m_1 N_1} + \frac{k_0 N_0^2}{1 + m_0 N_0} \\ \frac{dN_2}{dt} &= -\gamma N_2 + \beta_2 N_1 + \frac{c_1 N_1^2}{1 + m_1 N_1}. \end{aligned}$$

In the dynamics, the time variable t is in units of days, N_0 represents the stem cell population, N_1 the semi-differentiated cell population and N_2 the fully differentiated cell population. For the dynamics we fix the initial conditions to be $N_0 = 1$, $N_1 = 100$, $N_2 = 100$ and consider a time-span of 100 days. The remaining coefficients are the independent variables with which we perform the sensitivity analysis. Their interpretation and recommended values are given in

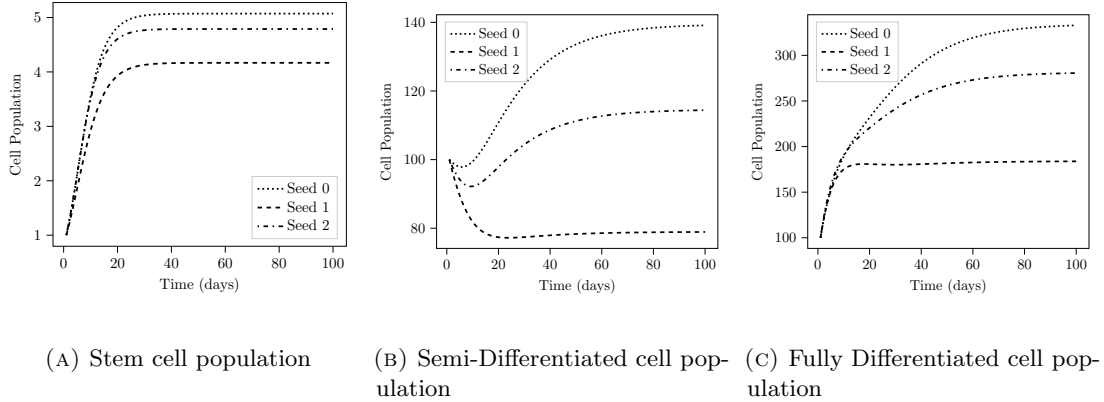


FIGURE 3. Visualization of ODE path with three randomly chosen parameters around the recommended values.

Table 11 of [40]. N_0 , the stem cell population, will be the dependent variable against which the sensitivity analysis is performed.

The domain we use is $\pm 10\%$ of the suggested values listed in [40]. To evaluate the differential equation we use the standard one-step explicit Euler scheme with a step size of 0.01, amounting to 10^4 steps per equation. To simulate noise in the observation of the final sample, we add noise with $\sigma = 10^{-3}$ which we found to be significantly more than the numerical error in simulating the dynamics. To get an understanding of how dynamics can change with different input parameters, we sample choose different parameters from the specified domain and plot them in Figure 3.

The dynamics do not have an analytic gradient easily available. Instead, we use central differences with a step-size of 10^{-11} to construct a gradient from the process without noise. We found the error due to machine precision and the discretization of the dynamics to be insignificant compared to the artificial noise added. To obtain the true Hessian we apply the same procedure to the estimated gradient values. The range of step-sizes for the gradient estimation is $\{3.16 \times 10^{-4}, 10^{-3}, 3.16 \times 10^{-3}, 10^{-2}, 3.16 \times 10^{-2}, 10^{-1}\}$. Since the number of variables is eleven, we use eCASG as described in Section 5. For Figure 4b the global model is fitted with 1,000 points.

6.2.3. *Sensitivity Analysis: Discussion.* Our method outperforms the forward difference based methods and the gradient estimates by the global model by up to an order of magnitude. More interestingly, our method appears to perform close to central differences. For the ODE problem, eCASG with the exact Hessian even outperforms central differences.

While outperforming central differences seems like a contradiction, as it supposed to be a best-case comparison, for some problems it may be the case that the layout of the difference vectors is not only good for a second-order approximation, but also a third order approximation. Hence, it may be that the specific sample set geometry also reduces the third-order error and hence improves upon central differences. Understanding how to purposefully distribute the sample set for a central-difference type gradient estimator is left for future work. Overall it is promising that the optimal sample set can achieve a comparable error as central difference with half the number of samples.

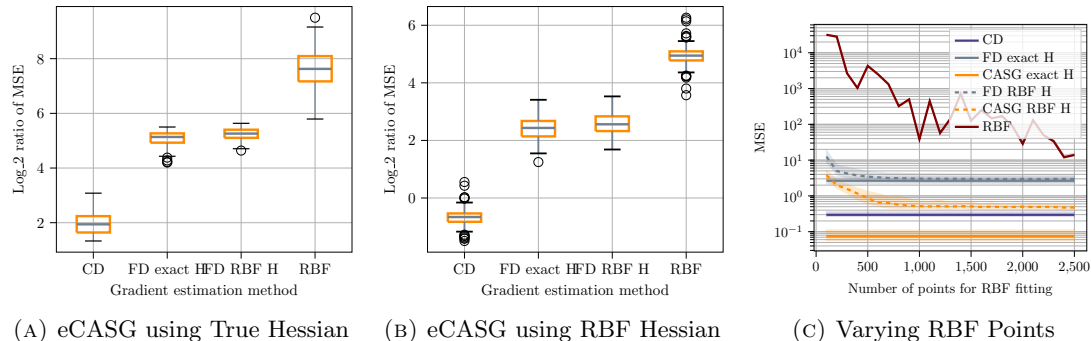


FIGURE 4. Comparison of gradient estimation methods for sensitivity analysis of cell differentiation in the colon with $\sigma = 10^{-3}$.

We now note the dependence on the number of sample points. While the box-plots are given a global model with 10,000 and 1,000 points, this corresponds to roughly 300 and 90 gradient estimates respectively. When a good understanding of the sensitivity of the system is needed, these are numbers which can be easily achieved. Furthermore, as seen in Figure 2c far fewer points suffice to obtain a strong gradient estimate.

6.3. Derivative Free Optimization. Another application in which gradient estimation is crucial is derivative free optimization (DFO). To compare the gradient estimation methods, we use the bench-marking methodology developed in [37] and test on a range of CUTEst problems [27]. For optimization we use a L-BFGS DFO framework from [4] which allows various gradient estimation methods to be plugged in while keeping everything else fixed.

Besides the methods considered for Sensitivity Analysis, we also consider the Adaptive Finite Difference (AFD) method [44]. AFD is based on forward differences and computes the lengths of difference vectors adaptively instead of using a global model. We consider AFD to be the state-of-the-art method for using finite differences in DFO as it has been shown to be more accurate and robust than comparable methods [44].

The sole hyperparameter h is set to 0.1, 0.01, and 0.001. While AFD is designed to not need such a parameter, to ensure fairness, in addition to leaving AFD with the default parameters we also assess it when upper-bounding the difference vectors by h as done for FD and CASG. To account for noise, for each hyperparameter we obtain ten random runs. We then set the optimal hyperparameter to be the one given by the random run which achieved the lowest function value. We then have ten random-runs with the chosen hyperparameter.

To provide some initial global understanding of the function, at initialization we sample $100 \times d$ points randomly in a cube of side-length two, where d is the dimension of the specific problem. During optimization, we save the function evaluations which happen as part of gradient estimation. While other points are evaluated as part of L-BFGS, adding them to the function evaluation history made the global model perform worse. When fitting the global model, we use the minimum number of $100 \times d$ and 1,000 data-points from the function evaluations along the optimization path. When using the the global model for gradient estimation, to obtain a function evaluation history we artificially construct a FD sample set with difference vector lengths of 0.1 after each gradient estimation by the global model. We then add these function evaluation to \mathcal{E} . Lastly, the smoothing parameter is set to 0.1.

In Figure 5 we plot the data-profiles [37] of each method. To create the plots, for each CUTEst problem P we let f_L^P be the lowest average function value achieved by any gradient estimation method for problem P , with the average being taken over the corresponding random runs. We then let the convergence criterion for the CUTEst problem be $(f(x_0^P) - f_L^P) \geq (1 - \tau)(f(x_0^P) - f(x_k^P))$, with x_0^P being the starting position for the problem, x_k^P the first point which satisfies the condition and τ being the tolerance. Notice that each random run has a natural convergence criterion associated via the problem it was executed on. The data-profile then plots for each gradient estimation method the fraction of random runs which achieved their corresponding convergence criterion within a certain number of function evaluations. We use the unit of simplex gradients, which is simply the number of total function evaluations divided by the dimension of the problem.

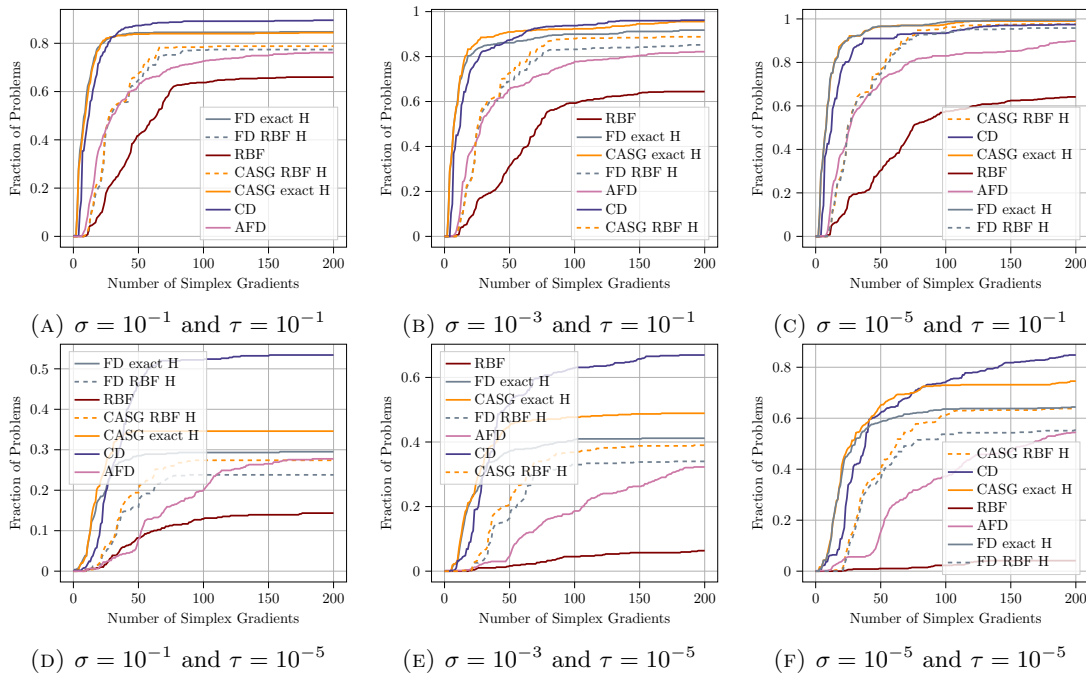


FIGURE 5. Data profiles for L-BFGS using various gradient estimation methods with noise levels $10^{-1}, 10^{-3}$ and 10^{-5} . The top row are the profiles with $\tau = 10^{-1}$, associated with approximate convergence. The bottom row is $\tau = 10^{-5}$, under which the convergence criterion is only satisfied if a random run is able to get very close to the lowest achievable function value.

In Figure 5 the lines for methods which use the global methods are shifted by ten simplex gradient evaluations due to the initialization data. In some cases the initialization data may not be considered as part of the expense of optimization as the function may have been evaluated at various locations already. In which case the graph would be shifted over by ten simplex gradient evaluations, improving our method in terms of budget required.

6.3.1. *DFO: Discussion.* In Figure 5 we observe that when $\tau = 10^{-1}$, many of the methods perform similarly, as the convergence criterion is relaxed. So, if an approximate solution is

required then CASG and FD may suffice. Especially when the initialization data for the global model is not included, the methods using the global model may be favorable, as fewer evaluations than CD may be necessary.

However, when $\tau = 10^{-5}$ more accurate methods perform significantly better. When the true Hessian is used, at first both CASG and FD perform better, since per gradient estimate fewer evaluations are needed. However, there comes a point where the lines intersect with CD, as then the methods can not match the accuracy of CD.

We also observe that CASG with the global model outperforms all other forward difference based models. Specifically, when higher accuracy is needed the gap between the two methods is significant. Additionally, even standard forward differences using our framework tends to outperform AFD, implying that our framework which uses a global model may be more suited for DFO.

We do note that AFD tends to continue improving after 200 steps. As the other methods have already long obtained convergence, we decided on a comprise to show the initial variation while showing the approximate convergence of AFD. However, AFD does not outperform CASG even when more evaluations are used and tends to eventually become similar to FD using the global model framework.

Overall, CASG using the true Hessian far outperforms all other gradient estimation methods except for CD once enough function evaluations have been used. In practice only CASG with the global model framework can be used, which also outperforms all comparable methods. Importantly, CASG with the global model performs comparable to FD using the true Hessian. Hence, even if a better finite difference based method is developed, CASG with our framework should provide an upper-bound in performance.

7. CONCLUSION

We studied the optimal sample set for the simplex gradient and introduced a framework which makes our method useful in practice. We showed that the improvement in CASG comes from aligning the sample set along the directions with lowest curvature. We numerically found that CASG consistently outperforms optimal forward differences and hence will improve on any forward difference based methods in practice. Additionally, we found CASG to often be closer in performance to central differences than forward differences, even though central differences needs twice as many function evaluations.

The implications are that in many applications in which function evaluations are costly, CASG may be used as an immediate improvement to forward difference type schemes, or drop-in for central difference methods, which would otherwise require twice the number of function evaluations. In settings where each function evaluation requires an expensive simulation or completion of a process, reducing the number of evaluations required by a factor of two will be substantial. Overall, CASG and eCASG, in conjunction with our global model framework, are highly competitive gradient estimators which may be used as a replacement for many numerical differentiation methods in real-world applications.

REFERENCES

- [1] Karsten Ahnert and Markus Abel. Numerical differentiation of experimental data: local versus global methods. *Computer Physics Communications*, 177(10):764–774, 2007.
- [2] Russell R Barton. Computing forward difference derivatives in engineering optimization. *Engineering optimization*, 20(3):205–224, 1992.
- [3] Atılım Gunes Baydin, Barak A Pearlmutter, Alexey Andreyevich Radul, and Jeffrey Mark Siskind. Automatic differentiation in machine learning: a survey. *Journal of Machine Learning Research*, 18:1–43, 2018.

- [4] Albert S Berahas, Richard H Byrd, and Jorge Nocedal. Derivative-free optimization of noisy functions via quasi-newton methods. *SIAM Journal on Optimization*, 29(2):965–993, 2019.
- [5] Albert S Berahas, Liyuan Cao, Krzysztof Choromanski, and Katya Scheinberg. Linear interpolation gives better gradients than gaussian smoothing in derivative-free optimization. *arXiv preprint arXiv:1905.13043*, 2019.
- [6] Albert S Berahas, Liyuan Cao, Krzysztof Choromanski, and Katya Scheinberg. A theoretical and empirical comparison of gradient approximations in derivative-free optimization. *Foundations of Computational Mathematics*, 22(2):507–560, 2022.
- [7] S.. Bhatnagar, HL Prasad, and LA Prashanth. *Stochastic Recursive Algorithms for Optimization: Simultaneous Perturbation Methods*. Springer, 2013.
- [8] Sujay Bhatt, Alec Koppel, and Vikram Krishnamurthy. Policy gradient using weak derivatives for reinforcement learning. pages 5531–5537. IEEE, 2019 IEEE 58th Conference on Decision and Control (CDC), 2019.
- [9] Adam Blakney and Jingyi Zhu. A comparison of the finite difference and simultaneous perturbation gradient estimation methods with noisy function evaluations. pages 1–6. IEEE, 2019 53rd Annual Conference on Information Sciences and Systems (CISS), 2019.
- [10] Vivek S Borkar, Vikranth R Dwaracherla, and Neeraja Sahasrabudhe. Gradient estimation with simultaneous perturbation and compressive sensing. *The Journal of Machine Learning Research*, 18(1):5910–5936, 2017.
- [11] RCM Brekelmans, LT Driessen, HJM Hamers, and Dick den Hertog. Gradient estimation using lagrange interpolation polynomials. *Journal of optimization theory and applications*, 136(3):341–357, 2008.
- [12] RCM Brekelmans, LT Driessen, HJM Hamers, and D den Hertog. Gradient estimation schemes for noisy functions. *Journal of Optimization Theory and Applications*, 126(3):529–551, 2005.
- [13] O Bruno and D Hoch. Numerical differentiation of approximated functions with limited order-of-accuracy deterioration. *SIAM Journal on Numerical Analysis*, 50(3):1581–1603, 2012.
- [14] Richard L Burden, J Douglas Faires, and Annette M Burden. *Numerical analysis*. Cengage learning, 2015.
- [15] E.W. Cheney and W.A. Light. *A Course in Approximation Theory*. Graduate studies in mathematics. American Mathematical Society, 2009.
- [16] Andrew R Conn, Katya Scheinberg, and Luís N Vicente. Geometry of interpolation sets in derivative free optimization. *Mathematical programming*, 111:141–172, 2008.
- [17] Andrew R Conn, Katya Scheinberg, and Luis N Vicente. Geometry of sample sets in derivative-free optimization: polynomial regression and underdetermined interpolation. *IMA journal of numerical analysis*, 28(4):721–748, 2008.
- [18] Ian Coope and Rachael Tappenden. Efficient calculation of regular simplex gradients. *Computational Optimization and Applications*, 72:561–588, 2019.
- [19] Jane Cullum. Numerical differentiation and regularization. *SIAM Journal on numerical analysis*, 8(2):254–265, 1971.
- [20] AL Custódio, JE Dennis, and Luís Nunes Vicente. Using simplex gradients of nonsmooth functions in direct search methods. *IMA journal of numerical analysis*, 28(4):770–784, 2008.
- [21] Ana Luísa Custódio and Luís Nunes Vicente. Using sampling and simplex derivatives in pattern search methods. *SIAM Journal on Optimization*, 18(2):537–555, 2007.
- [22] Germund Dahlquist and Åke Björck. *Numerical methods*. Courier Corporation, 2003.
- [23] Ronald Aylmer Fisher. Design of experiments. *British Medical Journal*, 1(3923):554, 1936.
- [24] Bengt Fornberg. Generation of finite difference formulas on arbitrarily spaced grids. *Mathematics of computation*, 51(184):699–706, 1988.
- [25] Philip E. Gill, Walter Murray, Michael A. Saunders, and Margaret H. Wright. Computing forward-difference intervals for numerical optimization. *SIAM Journal on Scientific and Statistical Computing*, 4(2):310–321, 1983.
- [26] Philip E Gill, Walter Murray, and Margaret H Wright. *Practical optimization*. SIAM, 2019.
- [27] Nicholas IM Gould, Dominique Orban, and Philippe L Toint. Cutest: a constrained and unconstrained testing environment with safe threads for mathematical optimization. *Computational optimization and applications*, 60:545–557, 2015.
- [28] Christian Gourieroux, Jean-Paul Laurent, and Olivier Scaillet. Sensitivity analysis of values at risk. *Journal of empirical finance*, 7(3-4):225–245, 2000.
- [29] Andreas Griewank et al. On automatic differentiation. *Mathematical Programming: recent developments and applications*, 6(6):83–107, 1989.

- [30] Martin Hanke and Otmar Scherzer. Inverse problems light: numerical differentiation. *The American Mathematical Monthly*, 108(6):512–521, 2001.
- [31] Warren Hare and Gabriel Jarry-Bolduc. Calculus identities for generalized simplex gradients: Rules and applications. *SIAM Journal on Optimization*, 30(1):853–884, 2020.
- [32] Warren Hare, Gabriel Jarry-Bolduc, and Chayne Planiden. Error bounds for overdetermined and underdetermined generalized centred simplex gradients. *IMA Journal of Numerical Analysis*, 42(1):744–770, 2022.
- [33] Matthew D Johnston, Carina M Edwards, Walter F Bodmer, Philip K Maini, and S Jonathan Chapman. Examples of mathematical modeling: tales from the crypt. *Cell cycle*, 6(17):2106–2112, 2007.
- [34] David A Kendrick. Stochastic control for economic models: past, present and the paths ahead. *Journal of economic dynamics and control*, 29(1-2):170–171, 2005.
- [35] Ian Knowles and Robert J Renka. Methods for numerical differentiation of noisy data. *Electron. J. Differ. Equ*, 21:235–246, 2014.
- [36] Douglas C Montgomery. *Design and analysis of experiments*. John wiley & sons, 2017.
- [37] Jorge J Moré and Stefan M Wild. Benchmarking derivative-free optimization algorithms. *SIAM Journal on Optimization*, 20(1):172–191, 2009.
- [38] Jorge J Moré and Stefan M Wild. Estimating derivatives of noisy simulations. *ACM Transactions on Mathematical Software (TOMS)*, 38(3):1–21, 2012.
- [39] Robin L Plackett and J Peter Burman. The design of optimum multifactorial experiments. *Biometrika*, 33(4):305–325, 1946.
- [40] George Qian and Adam Mahdi. Sensitivity analysis methods in the biomedical sciences. *Mathematical biosciences*, 323:108306, 2020.
- [41] Rommel G Regis. The calculus of simplex gradients. *Optimization Letters*, 9(5):845–865, 2015.
- [42] Katya Scheinberg. Finite difference gradient approximation: To randomize or not? *INFORMS Journal on Computing*, 2022.
- [43] John Schulman, Nicolas Heess, Theophane Weber, and Pieter Abbeel. Gradient estimation using stochastic computation graphs. *Advances in Neural Information Processing Systems*, 28, 2015.
- [44] Hao-Jun Michael Shi, Yuchen Xie, Melody Qiming Xuan, and Jorge Nocedal. Adaptive finite-difference interval estimation for noisy derivative-free optimization. *SIAM Journal on Scientific Computing*, 44(4):A2302–A2321, 2022.
- [45] James C Spall. An overview of the simultaneous perturbation method for efficient optimization. *Johns Hopkins apl technical digest*, 19(4):482–492, 1998.
- [46] James C Spall et al. Multivariate stochastic approximation using a simultaneous perturbation gradient approximation. *IEEE transactions on automatic control*, 37(3):332–341, 1992.
- [47] Rajan Suri. Infinitesimal perturbation analysis for general discrete event systems. *Journal of the ACM (JACM)*, 34(3):686–717, 1987.
- [48] Floris Van Breugel, J Nathan Kutz, and Bingni W Brunton. Numerical differentiation of noisy data: A unifying multi-objective optimization framework. *IEEE Access*, 8:196865–196877, 2020.
- [49] Pauli Virtanen, Ralf Gommers, Travis E. Oliphant, Matt Haberland, Tyler Reddy, David Cournapeau, Evgeni Burovski, Pearu Peterson, Warren Weckesser, Jonathan Bright, Stéfan J. van der Walt, Matthew Brett, Joshua Wilson, K. Jarrod Millman, Nikolay Mayorov, Andrew R. J. Nelson, Eric Jones, Robert Kern, Eric Larson, C J Carey, İlhan Polat, Yu Feng, Eric W. Moore, Jake VanderPlas, Denis Laxalde, Josef Perktold, Robert Cimrman, Ian Henriksen, E. A. Quintero, Charles R. Harris, Anne M. Archibald, Antônio H. Ribeiro, Fabian Pedregosa, Paul van Mulbregt, and SciPy 1.0 Contributors. SciPy 1.0: Fundamental Algorithms for Scientific Computing in Python. *Nature Methods*, 17:261–272, 2020.
- [50] Yorai Wardi, Christos G Cassandras, and Xi-Ren Cao. Perturbation analysis: a framework for data-driven control and optimization of discrete event and hybrid systems. *Annual Reviews in Control*, 45:267–280, 2018.
- [51] Ting Wei and YC Hon. Numerical differentiation by radial basis functions approximation. *Advances in Computational Mathematics*, 27(3):247–272, 2007.
- [52] Ronald J Williams. Simple statistical gradient-following algorithms for connectionist reinforcement learning. *Machine learning*, 8(3):229–256, 1992.
- [53] JC Zhang and MA Styblinski. Design of experiments approach to gradient estimation and its application to cmos circuit stochastic optimization. pages 3098–3101. IEEE, 1991., IEEE International Symposium on Circuits and Systems, 1991.

APPENDIX A. APPENDIX: PROOFS

A.1. Taylor Bound. *Proof.* [Proof of Proposition 3] By Taylor's Theorem for a fixed x_0 and bounded x_i (which we have due to the assumption $\|S\|_2 \leq h$) we have

$$\begin{aligned} f(x_i) - f(x_0) &= (\nabla f(x_0))^T s_i + \frac{1}{2} s_i^T \nabla^2 f(x_0) s_i + O(\|S\|_2^3) \\ \rightarrow \delta \tilde{\mathbf{f}} &= S^T \nabla f(x_0) + \frac{1}{2} \text{diag}(S^T \nabla^2 f(x_0) S) + \mathbf{O}(\|S\|_2^3) \\ \rightarrow \nabla_S f(x_0) &= S^{-T} \delta \tilde{\mathbf{f}} = \nabla f(x_0) + \frac{1}{2} S^{-T} \text{diag}(S^T \nabla^2 f(x_0) S) + \mathbf{O}(\|S\|_2^2). \end{aligned}$$

$$\begin{aligned} \|\nabla_S f(x_0) - \nabla f(x_0)\|_2^2 &= \|S^{-T} \delta \tilde{\mathbf{f}} - \nabla f(x_0)\|_2^2 \\ &= \left\| \frac{1}{2} S^{-T} \text{diag}(S^T \nabla^2 f(x_0) S) + \mathbf{O}(\|S\|_2^2) \right\|_2^2 \\ &= \frac{1}{4} \|S^{-T} \text{diag}(S^T \nabla^2 f(x_0) S)\|_2^2 + O(\|S\|_2^3). \end{aligned}$$

□

A.2. Poofs for Theorem 6.

A.2.1. *Proof of Proposition 8.* We first present the following results.

Lemma 17. *Given an invertible matrix S with singular value decomposition $S = U\Sigma V^T$, diagonal matrix D and real number σ we have*

$$\begin{aligned} &\frac{1}{4} \|S^{-T} [s_i^T D s_i]_{1 \leq i \leq d}^T\|_2^2 + \sigma^2 \|S^{-1}\|_F^2 + \sigma^2 \|S^{-T} \mathbf{1}\|_2^2 \\ &\geq \frac{1}{4} \frac{1}{\Sigma_{max}^2} \|[s_1^T D s_1, \dots, s_d^T D s_d]^T\|_2^2 + \sigma^2 \sum_{i=1}^d \frac{1}{\Sigma_i^2} + \sigma^2 \frac{d}{\Sigma_{max}^2}. \end{aligned}$$

The lower bound is achieved if both $[s_1^T D s_1, \dots, s_d^T D s_d]^T$ and $\mathbf{1}$ are right singular vectors, i.e. columns of V , associated with the singular value Σ_{max} .

Proof. This is immediate by noticing that for any vector v and matrix A we have $\|Av\|_2 \geq \sigma_{min} \|v\|_2$, and that the Frobenius norm is the sum of the squares of singular values. Clearly, $\|Av\|_2 = \sigma_{min} \|v\|_2$ when v is the right singular vector associated with the smallest singular value of A . □

Lemma 18. *Let $c \in \mathbb{R}_+$, then the solution w^* to*

$$\begin{aligned} &\min_{w \in \mathbb{R}^d} \|w\|_2^2 \\ &s.t. \quad \sum_{i=1}^d w_i = c \end{aligned}$$

is given by $w_i^* = \frac{c}{d}$ for $1 \leq i \leq d$.

Proof. The proof is a simple application of Lagrange multipliers. □

Lemma 19. *Let V be an orthogonal matrix and D a diagonal matrix. Then for any orthogonal matrix U and diagonal matrix Σ we have*

$$\|[v_i^T \Sigma U^T D U \Sigma v_i]_{1 \leq i \leq d}^T\|_2^2 \geq \frac{1}{d} \text{tr}(\Sigma U^T D U \Sigma)^2.$$

Proof. Due to the cyclic property of the trace we have

$$\begin{aligned} \sum_{i=1}^d v_i^T \Sigma U^T D U \Sigma v_i &= \text{tr}(V \Sigma U^T D U \Sigma V^T) \\ &= \text{tr}(\Sigma U^T D U \Sigma). \end{aligned}$$

By Lemma 18 the vector $w^* \in \mathbb{R}^d$ which minimizes $\|w\|_2^2$ under the constraint $\sum_{i=1}^d w_i = \text{tr}(\Sigma U^T D U \Sigma)$ is given by $w_i^* = \frac{1}{d} \text{tr}(\Sigma U^T D U \Sigma)$. \square

Proof. [Proof of Proposition 8] Consider the case when $hI \succeq \Sigma \succ 0$. Otherwise, the functions both evaluate to ∞ and the bound trivially holds on the extended real number line. Letting $s_i^T D s_i = v_i^T \Sigma U^T D U \Sigma v_i$ and combining Lemma 17 and 19 we have that

$$\begin{aligned} l(U, \Sigma, V) &\geq \frac{1}{4} \frac{1}{\Sigma_{max}^2} \|[s_1^T D s_1, \dots, s_d^T D s_d]^T\|_2^2 + \sigma^2 \sum_{i=1}^d \frac{1}{\Sigma_i^2} + \sigma^2 \frac{1}{\Sigma_{max}^2} \|\mathbf{1}\|_2^2 \\ &\geq \frac{1}{4d\Sigma_{max}^2} \text{tr}(\Sigma U^T D U \Sigma)^2 + \sigma^2 \sum_{i=1}^d \frac{1}{\Sigma_i^2} + \sigma^2 \frac{d}{\Sigma_{max}^2} \end{aligned}$$

which by taking the minimum over V on both sides completes the proof. \square

A.2.2. *Proof of Proposition 9.* We first consider the form of U' for any given Σ . Since only $a(U, \Sigma)$ depends on U , it suffices to focus on this term.

Lemma 20. *Fix a diagonal matrix Σ and we have that*

- *the extrema of $a(U, \Sigma)$ are given by the set of permutation matrices and,*
- *the extrema of $a(U, \Sigma)^2$ are given by the set of permutation matrices and all matrices U_0 such that $a(U_0, \Sigma) = 0$.*

Proof. For $a(U, \Sigma)$ and $a(U, \Sigma)^2$, the minimum with respect to U under the orthogonality constraint $U^T U = I$ is achieved since the objective function is continuous and the set of orthogonal matrices is compact.

The Lagrangian for minimizing $a(U, \Sigma)$ is given by $\mathcal{L}(U, \mu) = \text{tr}(\Sigma U^T D U \Sigma) - \sum_{i,j} \mu_{ij} (u_i^T u_j - \delta_{ij})$. Taking the gradient with respect to U and setting to zero we obtain

$$2U^T D V \Sigma^2 = (\mu + \mu^T).$$

Due to $\mu + \mu^T$ we have the symmetry relation

$$U^T D U \Sigma^2 = \Sigma^2 U^T D U$$

which means that $U^T D U$ and Σ^2 commute, implying that they are simultaneously diagonalizable. Therefore, Σ^2 and $U^T D U$ share the same eigenvectors.

Since Σ^2 is diagonal, it has the standard basis vectors as eigenvectors. The set of orthogonal matrices that represent the standard basis are permutation matrices P . Hence, we want that $P U^T D U P^T = D$ which can only happen when $P U^T = I$ and hence $U = P$. Hence, U has to be a permutation matrix.

For minimizing $a^2(U, \Sigma)$ we have that by setting the gradient of the associated Lagrangian to zero provides

$$4\text{tr}(\Sigma U^T D U \Sigma) U^T D U \Sigma^2 = (\mu + \mu^T).$$

If it exists, the equation can be satisfied by an orthogonal matrix U_0 such that $\text{tr}(\Sigma U^T D U \Sigma) = a(U_0, \Sigma) = 0$. Otherwise, just as before we see that $U^T D U$ and Σ^2 commute, implying that U has to be a permutation matrix. \square

Remark 4. Letting $U_{max}(\Sigma)$ and $U_{min}(\Sigma)$ be the permutation matrix which respectively maximize and minimize $a(U, \Sigma)$ for a given Σ , if there exists U_0 such that $a(U_0, \Sigma) = 0$ it immediately follows that

$$a(U_{max}(\Sigma), \Sigma) \geq 0 \geq a(U_{min}(\Sigma), \Sigma).$$

By showing that we can discard U_0 , which means that we only have to work with permutation matrices, we can significantly simplify the problem. To show this, we first present the following result which tells us that for the optimal (U', Σ') the sign of $a(\Sigma', U_{ext})$ is the same for all extrema U_{ext} .

Lemma 21. Without loss of generality assume that $\sum_{i=1}^d D_i \geq 0$ and let (U', Σ') be optimal. Then for all extrema U_{ext}

- if $\sum_{i=1}^d D_i = 0$ then $a(\Sigma', U_{ext}) = 0$ and $\Sigma' = hI$ and $U' = I$;
- if $\sum_{i=1}^d D_i > 0$ then $a(\Sigma', U_{ext}) \geq 0$.

Proof. We proceed by cases.

(i) Letting $\sum_{i=1}^d D_i = 0$ we have that for any Σ and all extrema U_{ext}

$$\frac{1}{4\Sigma_{max}^2} \frac{a(U_{ext}, \Sigma)}{d} + \sigma^2 \sum_{i=1}^d \frac{1}{\Sigma_i^2} + \sigma^2 \frac{1}{\Sigma_{max}^2} d \geq \sigma^2 \sum_{i=1}^d \frac{1}{\Sigma_i^2} + \sigma^2 \frac{1}{\Sigma_{max}^2} d.$$

To minimize $\sigma^2 \sum_{i=1}^d \frac{1}{\Sigma_i^2} + \sigma^2 \frac{1}{\Sigma_{max}^2} d$ we want to maximize each element along the diagonal Σ , which is achieved when $\Sigma = hI$. Hence, $\Sigma' = hI$ as this will minimize the loss for all extrema U_{ext} chosen. Specifically, I is a permutation matrix and hence $U' = I$.

(ii) Assume that $\sum_{i=1}^d D_i > 0$. If $D \succeq 0$ the result is immediate. Hence, assume that at least one entry of D is negative. For contradiction, assume that for Σ' we have $a(\Sigma', U_{min}) < 0$, where U_{min} is the permutation matrix which minimizes $a(\Sigma', U)$. For ease of notation and without loss of generality, we assume that Σ' is sorted such that $U_{min}(\Sigma') = I$. We proceed by showing that we can find $\Sigma \succeq \Sigma'$ which reduces the objective function leading to a contradiction.

For the proof we introduce some further notation. Let $I = \{i | D_i < 0\}$. We assign $c = (\sum_{i \in I} |D_i| (\Sigma'_i)^2) / (\sum_{i \in I} |D_i|)$ where $\sqrt{c} \leq h$ since by assumption $\Sigma' \preceq hI$. Set $J = \{j | (\Sigma'_j)^2 \leq c, j \notin I\}$. Lastly, define a function $\Sigma(\alpha) : [0, 1] \rightarrow \mathbb{R}^{d \times d}$ such that

$$(\Sigma(\alpha))_i = \begin{cases} \Sigma_i + \alpha(\sqrt{c} - \Sigma_i) & \text{if } i \in J \\ \Sigma_i & \text{otherwise.} \end{cases}$$

We show that given this construction $a(\Sigma(1), U_{min}) \geq 0 > a(\Sigma(0), U_{min})$. The lower bound is immediate. Letting $\alpha = 1$

$$\begin{aligned} \sum_{i \notin I} D_i (\Sigma'_i(1))^2 &= \sum_{i \in J, i \notin I} c D_i + \sum_{i \notin J, i \notin I} D_i (\Sigma'_i)^2 \\ &\geq c \sum_{i \notin I} D_i \\ &\geq \sum_{i \in I} |D_i| (\Sigma'_i)^2. \end{aligned}$$

The last step follows from $\sum_{i \in I} |D_i| < \sum_{i \notin I} |D_i|$ due to the assumption $\sum_{i=1}^d D_i > 0$. By the above $\sum_{i \notin I} D_i (\Sigma'_i(1))^2 - \sum_{i \in I} |D_i| (\Sigma'_i)^2 \geq 0$ which by definition implies $a(\Sigma(1), U_{min}) \geq 0$.

By the continuity of $a(\Sigma(\cdot), U_{min})$ and the above, we have that by the intermediate value theorem there exists an $\alpha_0 \in (0, 1]$ such that $a(\Sigma(\alpha_0), U_{min}) = 0$. Combined with the fact that $\Sigma(\alpha_0) \succeq \Sigma'$ the objective function has been strictly decreased by using $\Sigma(\alpha_0)$ leading to a contraction. \square

Proof. [Proof of Proposition 9] If $\sum_i D_i = 0$ we are immediately done as by the first part of Lemma 21 $U = I$. When $\sum_i D_i > 0$, we have that $a(\Sigma', U') \geq 0$ which implies that even if U_0 exists

$$a(U_{max}(\Sigma), \Sigma) \geq a(U_0(\Sigma), \Sigma) \geq a(U_{min}(\Sigma), \Sigma) \geq 0$$

and hence U_{min} is optimal. If U_0 does not exist, then trivially $U' = U_{min}$. If U_{min} is not the identity matrix, we can permute U_{min} and any Σ without changing the objective function. Hence, $U' = I$ and $\Sigma' = \arg \min_{\Sigma} \underline{l}(I, \Sigma)$. \square

A.2.3. Proof of Proposition 10. Proof. Since Σ' is assumed to be a solution, $\Sigma' \succ 0$. We proceed by showing that the terms in the respective objective functions $l(U', \Sigma', V')$ and $\underline{l}(U', \Sigma')$ can be matched up and shown to be equal. Let $S' = \Sigma'(V')^T$, recalling that $U' = I$.

To show that the first term of the objective functions are equal note that

$$\begin{aligned} (s'_i)^T D s'_i &= (v'_i)^T \Sigma' D \Sigma' v'_i \\ &= \sum_{j=1}^d (V'_{i,j})^2 D_j (\Sigma'_j)^2 \\ &= \frac{1}{d} \sum_{j=1}^d D_j (\Sigma'_j)^2 && \text{Due to } V \text{ being the Hadamard matrix.} \\ &= \frac{1}{d} \text{tr}((\Sigma')^T D \Sigma') = \frac{1}{d} a(U', \Sigma'). \end{aligned}$$

It then follows that $[(s'_1)^T D s'_1, \dots, (s'_n)^T D s'_n]^T = \frac{1}{d} a(U', \Sigma') \mathbf{1}$. Since $V' = M_k$, $\mathbf{1}$ is the right singular vector of S' associated with Σ_{max} . Hence, by Lemma 17 we have that $\frac{1}{4} \|S^{-T} [s'_i^T D s'_i]_{1 \leq i \leq d}^T\|_2^2 = \frac{1}{4d(\Sigma'_{max})^2} a(U', \Sigma')^2$.

The second terms are trivially equal since the Frobenius norm is always the sum of the squares of the singular values. The third terms are equivalent as by Lemma 17, as similarly to the first term, $\mathbf{1}$ is the right singular vector associated with the largest singular value as . \square

A.3. Proofs for Proposition 7. For the following proofs we write $l(\lambda) := l(I, \text{diag}(\lambda), V^*) = \underline{l}(I, \text{diag}(\lambda))$. More specifically

$$l(\lambda) := \begin{cases} \frac{(\sum_{i=1}^d D_i \lambda_i^2)^2}{4d \lambda_{max}^2} + \sigma^2 \sum_{i=0}^d \frac{1}{\lambda_i^2} + \sigma^2 \frac{1}{\Sigma_{max}^2} d & \text{if } hI \succeq \lambda \succ 0 \\ \infty & \text{otherwise.} \end{cases}$$

Hence, our objective is to find $\lambda^* = \arg \min_{\lambda} l(\lambda)$. We will also use l_A which we define in Section 4.4.1.

A.3.1. *Proof of Proposition 11. Proof.* Define $K = \{i | D_i \leq 0\}$ for which the complement is given by $K^c = \{i | D_i > 0\}$. We first show that $\lambda_i = h^2$ for $D_i \leq 0$. Assume for contradiction that for some $1 \leq i \leq d$ with $D_i \leq 0$ we have $\lambda_i^* < h^2$. Now, define the function $\lambda(\alpha) \in \mathbb{R}^d$ for $\alpha \in [0, 1]$ as

$$\lambda_i(\alpha) = \begin{cases} h^2 & \text{if } i \in K \text{ or } \lambda_i^* + \alpha h^2 \geq h^2, \\ \lambda_i^* + \alpha h^2 & \text{otherwise.} \end{cases}$$

Given this definition $\lambda(\alpha) \succ \lambda^*$ for any chosen α value. Hence, the noise error component of the objective function will have strictly decreased. To complete the proof, we show that there exists an α^* for which the approximation error does not increase.

By Lemma 21 and the assumption that $\sum_{i=1}^d D_i \geq 0$ we know that for the optimal λ^* we have $\sum_{i=1}^d D_i \lambda_i^* \geq 0$. If instead of λ^* we use $\lambda(0)$ and $\sum_{i=1}^d D_i \lambda(0) \geq 0$ then we immediately know that we did not increase the approximation error. This is because now $\lambda_{max} = h^2$, placing a larger quantity in the denominator, and we made the λ_i corresponding to $D_i \leq 0$ larger which results in adding a larger negative quantity to the numerator, i.e.

$$\begin{aligned} \sum_{i=1}^d \lambda_i^* D_i &\geq \sum_{i \in K} D_i h^2 + \sum_{i \in K^c} \lambda_i^* D_i \\ &= \sum_{i=1}^d \lambda(0)_i D_i \geq 0. \end{aligned}$$

If instead $\sum_{i=1}^d D_i \lambda(0) \leq 0$ we use the intermediate value theorem to find an α^* which makes the sum equal to zero. By the assumption $\sum_{i=1}^d D_i \geq 0$ and that $\lambda(1) = h^2$ it follows that $\sum_{i=1}^d D_i \lambda(1) \geq 0$. Hence, by the intermediate value theorem there exists an α^* such that $\sum_{i=1}^d D_i \lambda(\alpha^*) = 0$ which implies that the approximation error is now zero. Hence, under this α^* we could not have increased the approximation error.

We know that $\lambda_i^* = h^2$ for all $i \in K$. Since D is in increasing order, these terms will fill the first $|K|$ entries of λ . For the remainder we show that λ has to be in decreasing order by way of contradiction. Assume that there exist $i, j \in K^c$ with $i < j$ and $\lambda_i < \lambda_j$. We then define

$$s = \frac{D_i \lambda_i + D_j \lambda_j}{D_i + D_j}.$$

This is well-defined as $D_i, D_j > 0$ by assumption. Due to the assumption we have immediately that $D_j \lambda_j > D_i \lambda_i$ from which it then follows that $\frac{1}{\lambda_i} + \frac{1}{\lambda_j} > \frac{2}{s}$. Since $s(D_i + D_j) = \lambda_i D_i + \lambda_j D_j$, we did not change the approximation error. However, we reduced the noise error since $\frac{1}{\lambda_i} + \frac{1}{\lambda_j} > \frac{2}{s}$. So the objective function can be reduced by replacing λ_i and λ_j with s , leading to a contradiction. \square

A.3.2. *Proofs for Finding all Candidate Solutions.*

Lemma 22. *There exists $A \in \mathcal{P}(\{1, \dots, d\})$ such that $\lambda^* \in \lambda_A^*$.*

Proof. Let $A = \{i | \lambda_i^* = h^2\}$, i.e. the set of all indices of the global optimum at which the constraints are strict. Since λ^* is a minimizer of $l(\lambda)$, $h \succeq \lambda^* \succ 0$ and hence λ^* is finite and in the domain of $l_A(\lambda)$. Additionally, Proposition 11 implies $\lambda_1 = \lambda_{max}$. Hence, $l_A(\lambda^*) = l(\lambda^*)$. Since by Fermat's theorem for all differentiable functions on open sets a point is a local minima if and only if it is a stationary point, it suffices to show that λ^* is a local minimum of $l_A(\lambda)$.

For this, note that for any in the domain of l_A we have $l_A(\lambda) \geq l(\lambda^{(A)})$. Since λ^* is a minimizer of $l(\lambda)$ and the two functions coincide there, it follows that λ^* is a local minimum of l_A as well and hence $\lambda^* \in \lambda_A^*$. \square

Proof. [Proof of Proposition 12] By Lemma 22 we know that there exists an active set for which one of the solutions provides the minimizer λ^* . Now, assume for contradiction that there does not exist $J \in \{|K|, \dots, d\}$ such that $\lambda^* \in \lambda_{A_J}^*$. Then, there has to either exist indices $i < j < k$ such that $\lambda_i^* = \lambda_k^* = h^2$ but $\lambda_j^* < h^2$ or an index $1 \leq l \leq |K|$ such that $\lambda_l < h^2$. However, by Proposition 11 we know that λ^* is decreasing and that the first $|K|$ entries have to be set to h^2 . \square

Proof. [Proof of Proposition 13] Let $a = \sum_{i \notin A} D_i \lambda_i + h^2 \sum_{i \in A} D_i$ and $\mathbb{1}$ be the indicator function. Then the stationary points are simply all the points which satisfy

$$(A.1) \quad \frac{\partial l_A(\lambda)}{\partial \lambda_1} = \mathbb{1}(1 \notin A) \left(\frac{D_1}{2d\lambda_1} a - \frac{1}{4d\lambda_1^2} a^2 - \sigma^2 \frac{d+1}{\lambda_1^2} \right) = 0$$

$$(A.2) \quad \frac{\partial l_A(\lambda)}{\partial \lambda_i} = \mathbb{1}(i \notin A) \left(\frac{D_i}{2d\lambda_1} a - \sigma^2 \frac{1}{\lambda_i^2} \right) = 0.$$

To manipulate the above equations we note that if not all constraints are set, i.e. $|A| < d$, it holds that $a > 0$ for every stationary point. This is because a is non-negative due to Lemma 21 and $a \neq 0$ as otherwise the stationary point can not exist since Equation A.2 can not be satisfied. It also holds that $D_i > 0$ for all $i \notin A$, as is immediate by the assumption that $K \subseteq A$. The result then follows by simple algebra. \square

The following Lemmas prove Proposition 14 by splitting it into two cases.

Lemma 23. *When the active set A_J is empty then the unique non-negative solution to a as given by the equations in Proposition 13 is*

$$a = \sqrt{2} \left(\frac{d\sigma^2}{D_1} \left(K \sqrt{8D_1(d+1) + K^2} + 2D_1(d+1) + K^2 \right) \right)^{1/2}$$

with $K = \sum_{i=2}^d \sqrt{D_i}$.

Proof. We rewrite $a = \sum_{i=1}^d D_i \lambda_i$ by plugging in λ_i to obtain

$$a = \sigma \sqrt{\frac{2d\lambda_1}{a}} \sum_{i=2}^d \sqrt{D_i} + \lambda_1 D_1.$$

Letting $K = \sum_{i=2}^d \sqrt{D_i}$, substituting λ_1 and simplifying we get

$$a = \frac{1}{a} \left(\sigma \sqrt{\frac{2d}{D_1} \left(\frac{a^2}{2} + 2\sigma^2 d(d+1) \right)} K + \left(\frac{a^2}{2} + 2\sigma^2 d(d+1) \right) \right).$$

The equation can be rewritten as solving for the roots of a fourth-order polynomial

$$\left(\frac{a^2}{2} - 2\sigma^2 d(d+1) \right)^2 - K^2 \frac{2d\sigma^2}{D_1} \left(\frac{a^2}{2} + 2\sigma^2 d(d+1) \right) = 0.$$

However, during the algebraic manipulation, additional roots may have been introduced. The potentially complex roots of the fourth order polynomial are given by two pairs

$$a'_1 = \pm\sqrt{2} \left(\frac{d\sigma^2}{D_1} \left(K\sqrt{8D_1(d+1) + K^2} + 2D_1(d+1) + K^2 \right) \right)^{1/2}$$

$$a'_2 = \pm\sqrt{2} \left(\frac{d\sigma^2}{D_1} \left(-K\sqrt{8D_1(d+1) + K^2} + 2D_1(d+1) + K^2 \right) \right)^{1/2}$$

which can be easily verified by plugging into the polynomial.

It is easy to verify that while a'_1 satisfies the original equation, a'_2 will not. Of the pair a'_1 , by assumption only the non-negative can be valid. Since all terms under square root are positive, the solution is also real and hence provides the unique solution

$$a = \sqrt{2} \left(\frac{d\sigma^2}{D_1} \left(K\sqrt{8D_1(d+1) + K^2} + 2D_1(d+1) + K^2 \right) \right)^{1/2}.$$

□

Lemma 24. *When the active set A_J is non-empty the solution for a given by the equations in Proposition 13 is given by*

$$a = \begin{cases} \frac{\sqrt[3]{\frac{2}{3}}c_2}{\sqrt[3]{\sqrt{3}\sqrt{27c_1^2 - 4c_2^3} + 9c_1}} + \frac{\sqrt[3]{\sqrt{3}\sqrt{27c_1^2 - 4c_2^3} + 9c_1}}{\sqrt[3]{18}} & \text{if } 27c_1^3 - 4c_2^3 \geq 0, \\ \cos(\theta/3)2\sqrt{\frac{c_2}{3}} & \text{otherwise,} \end{cases}$$

where $c_1 = \sigma\sqrt{\frac{2dh^2}{a}} \sum_{i=I+1}^d \sqrt{D_i}$ and $c_2 = \sum_{i=1}^I D_i h^2$.

For the proof we note the following Lemma

Lemma 25. *For $c_1 > 0$ and $c_2 \in \mathbb{R}$ there exists only one positive real root for the polynomial $f(x) = x^3 - c_2x - c_1$.*

Proof. Since $c_1 > 0$ and for any polynomial the negative of the order zero coefficient is the product of the roots, the product of the roots is positive and no root is zero. Furthermore, the second order term presents the sum of the roots, which is zero. For the sum of the roots to be zero, at least one root has to have a negative real component. For the product to be positive there has to exist another root with negative real component and one positive real root. Hence, there exists a unique real positive root. □

Proof. [Proof of Lemma 24] Plugging the equations for λ_i in $a = \sum_{i=1}^d D_i \lambda_i$ and after some simplification we get

$$a^{3/2} = \sigma\sqrt{2dh^2} \sum_{i \notin I} \sqrt{D_i} + \sqrt{a} \sum_{i \in I} D_i h^2.$$

Letting $c_1 = \sigma\sqrt{\frac{2dh^2}{a}} \sum_{i \notin I} \sqrt{D_i}$, $c_2 = \sum_{i \in I} D_i h^2$, and $x = \sqrt{a}$ the equation becomes

$$x^3 = c_1 + c_2x$$

when restricting $x \geq 0$. By Lemma 25 and $c_1 > 0$, there exists a unique positive x satisfying the equation which provides the solution \sqrt{a} .

The root is given by

$$x = \frac{\sqrt[3]{\frac{2}{3}c_2}}{\sqrt[3]{\sqrt{3}\sqrt{27c_1^2 - 4c_2^3} + 9c_1}} + \frac{\sqrt[3]{\sqrt{3}\sqrt{27c_1^2 - 4c_2^3} + 9c_1}}{\sqrt[3]{18}}.$$

We now show that the root is always well-defined, real, and non-negative. The root can be easily verified to be a root by plugging it into the polynomial.

To show well defined, real, and non-negative we split in two cases: $27c_1^2 - 4c_2^3 \geq 0$ and $27c_1^2 - 4c_2^3 < 0$.

i) Assume that $27c_1^2 - 4c_2^3 \geq 0$. It is well defined because then

$\sqrt[3]{\sqrt{3}\sqrt{27c_1^2 - 4c_2^3} + 9c_1} > 0$ since $c_1 > 0$. Furthermore, this quantity is real since every individual term is real. We now need to show non-negativeness. If $c_2 \geq 0$ it is trivial, hence assume $c_2 < 0$ for which we have

$$\begin{aligned} & \frac{\sqrt[3]{\frac{2}{3}c_2}}{\sqrt[3]{\sqrt{3}\sqrt{27c_1^2 - 4c_2^3} + 9c_1}} + \frac{\sqrt[3]{\sqrt{3}\sqrt{27c_1^2 - 4c_2^3} + 9c_1}}{\sqrt[3]{18}} \\ & > -\frac{\sqrt[3]{\frac{2}{3}|c_2|}}{\sqrt[3]{\sqrt{3}\sqrt{4|c_2|^3}}} + \frac{\sqrt[3]{\sqrt{3}\sqrt{4|c_2|^3}}}{\sqrt[3]{18}} = 0. \end{aligned}$$

ii) $27c_1^2 - 4c_2^3 < 0$ implies $c_2 > 0$ since $c_1 > 0$, which yields

$$\begin{aligned} \sqrt{3}\sqrt{27c_1^2 - 4c_2^3} + 9c_1 &= i\sqrt{3}\sqrt{4c_2^3 - 27c_1^2} + 9c_1 \\ &= r(\cos(\theta) + i\sin(\theta)) \\ &= re^{i\theta} = z \end{aligned}$$

where $\theta = \arccos(\frac{9c_1}{r})$ and after simplifying $r = \sqrt{12c_2^3}$. Since $c_2 > 0$ we have $r > 0$ and hence the root is well-defined. Substituting and simplifying yields that

$$x = \cos(\theta/3)2\sqrt{\frac{c_2}{3}}.$$

which shows that the root is real. The root is non-negative because $\cos(\theta) = \frac{9c_1}{r} > 0$ and hence $\theta \in (-\frac{\pi}{2}, \frac{\pi}{2})$, which implies that $\theta/3 \in (-\frac{\pi}{2}, \frac{\pi}{2})$ and $\cos(\theta/3) > 0$. \square

Proof. [Proof of Proposition 14] The result follows from combining Lemma 21 and 24. \square

A.3.3. *Proof of Proposition 15.* We prove the construction of λ^* in linear time. *Proof.* Assume for contradiction that there exists another index $J' > J$ for which $h^2 \geq \lambda_{A_{J'}}$ and $l_{A_J}(\lambda_{A_J}^*) \geq l_{A_{J'}}(\lambda_{A_{J'}})$. Since $\lambda_{A_{J'}}$ also satisfies the active set A_J we have that $l_{A_J}(\lambda_{A_{J'}}^*) \geq l_{A_J}(\lambda_{A_{J'}})$ implying that $\lambda_{A_{J'}}^*$ was not the global minimum. By Proposition 14 this non-uniqueness is a contradiction. The second part follows from Proposition 13 that $\lambda_{A_J}^*$ is decreasing from the $J + 1$ th entry on-wards when $J \geq 1$. Hence it suffices to only compute and check that the $J + 1$ th entry is less than h^2 , i.e. $h^2 \geq (\lambda_{A_J}^*)_{J+1}$ \square